CHARLES UNIVERSITY

Faculty of Pharmacy in Hradec Kralove

Department of Organic and Bioorganic Chemistry

OPTIMIZATION OF THE METHOD FOR QUANTIFICATION OF LIPIDS IN HUMAN CORNEOCYTE LIPID ENVELOPE

Diploma Thesis

Seyedmohammad Khatibi

Supervisor: PharmDr. Lukáš Opálka, Ph.D.

Consultant: RNDr. Martina Navrátilová, Ph.D.

Hradec Kralove 2024

Declaration

I declare that this thesis is my original work. All literature and other sources used during its preparation are listed in the bibliography and properly cited within the thesis. This work has not been used to obtain any other or the same degree.

In Hradec Králové 28 August 2024 Seyedmohammad Khatibi

Acknowledgments

I would like to express my sincere gratitude to my supervisor, PharmDr. Lukáš Opálka, Ph.D., for his professional guidance, expert advice, patience, willingness, and supportive attitude throughout the completion of this thesis. I also extend my thanks to all the staff of the Department of Organic and Bioorganic Chemistry for providing a pleasant working environment.

A special thanks goes to RNDr. Martina Navrátilová, Ph.D., whose notable patience and invaluable assistance with analyzing, processing results, creating graphs, preparing samples, and providing modification ideas were crucial to the success of this project.

Last but not least, I want to thank my family and friends for their tremendous support.

ABSTRACT

Charles University, Faculty of Pharmacy in Hradec Králové

Department of Organic and Bioorganic Chemistry

Candidate: Seyedmohammad Khatibi

Supervisor: PharmDr. Lukáš Opálka, Ph.D.

Consultant: RNDr. Martina Navrátilová, Ph.D.

Title of diploma thesis: Optimization of the method for quantification of lipids in human corneocyte lipid envelope

Ceramides are essential sphingolipids in the skin, playing crucial roles in barrier function and cellular regulation. This study aimed to optimize the isolation of covalently bound ceramides from the skin's *stratum corneum* by developing and refining extraction and saponification procedures. Specifically, the focus was on ceramide types NS (free lipids), OS, OH, OdS, and OP, obtained from samples of three healthy individuals.

Eight layers of the *stratum corneum* were collected from each participant and merged to form a composite sample. The isolation procedures were divided into three main steps: extraction of free lipids, purification of the remaining pellet, and saponification of covalently bound lipids. The procedures were systematically tested under varying conditions across seven experiments to determine the optimal parameters for ceramide extraction.

Initial experiments revealed that high temperatures during extraction and saponification led to significant degradation of covalently bound lipids. The first experiment, using high-temperature procedures, resulted in the complete destruction of covalently bound lipids. Subsequent experiments demonstrated that lower temperatures improved the stability of ceramides. In particular, with modified conditions including a bath temperature of 40°C for purification and 37°C for saponification, several ceramide types were successfully isolated. This approach revealed significant quantities of ceramide OS, ceramide OH, ceramide OdS, and ceramide OP. Ceramide NS was found in minor quantities, indicating the effective removal of free lipids.

Further refinement of conditions, which varied in saponification temperatures and times, showed that increased saponification time enhanced the extraction of OS and OdS ceramides. Specifically, longer saponification times improved the recovery of OS ceramides, while high temperatures adversely affected the stability of free lipids and some ceramides.

This study identified the critical role of temperature and washing/saponification times in optimizing ceramide extraction. Lower temperatures and extended washing and saponification times significantly improved the recovery of ceramide types OS, OdS, and OP, while high temperatures led to degradation. The optimized procedures outlined in this study provide a reliable method for isolating and analyzing ceramides, offering insights into their distribution and potential implications for skin health research.

Keywords: Ceramides, Sphingolipids, *Stratum corneum*, Lipid envelope, Covalently bound lipids, Lipid extraction, Saponification, Skin barrier, Lipid quantification, Temperature effects on lipids, Skin health research.

ABSTRAKT

Univerzita Karlova, Farmaceutická fakulta v Hradci Králové

Katedra organické a bioorganické chemie

Kandidát: Seyedmohammad Khatibi

Školitel: PharmDr. Lukáš Opálka, Ph.D.

Konzultant: RNDr. Martina Navrátilová, Ph.D.

Název diplomové práce: Optimalizace metody kvantifikace lipidů lidské korneocytální lipidové obálky

Ceramidy jsou esenciální sfingolipidy v kůži, které hrají klíčovou roli v bariérové funkci a buněčné regulaci. Cílem této studie bylo optimalizovat izolaci kovalentně vázaných ceramidů ze *stratum corneum* kůže prostřednictvím vývoje a zdokonalení extrakčních a saponifikačních postupů. Zaměření bylo konkrétně na ceramidy typu NS (volné lipidy), OS, OH, OdS a OP, získané ze vzorků tří zdravých jedinců.

Z každého dobrovolníka bylo odebráno osm vrstev *stratum corneum*, které byly spojeny do jednoho vzorku. Postupy izolace byly rozděleny do tří hlavních kroků: extrakce volných lipidů, čištění zbývající pelety a saponifikace kovalentně vázaných lipidů. Postupy byly systematicky testovány za různých podmínek v průběhu sedmi experimentů, aby byly stanoveny optimální parametry pro extrakci ceramidů.

Počáteční experimenty ukázaly, že vysoké teploty během extrakce a saponifikace vedly k významné degradaci kovalentně vázaných lipidů. První experiment, který využíval vysoké teploty, vedl k úplné destrukci kovalentně vázaných lipidů. Následující experimenty prokázaly, že nižší teploty zlepšily stabilitu ceramidů. Zejména při upravených podmínkách, které zahrnovaly teplotu lázně 40°C pro čištění a 37°C pro saponifikaci, bylo úspěšně izolováno několik typů ceramidů. Tento přístup odhalil významné množství ceramidu OS, ceramidu OH, ceramidu OdS a ceramidu OP. Ceramid NS byl nalezen v malém množství, což naznačuje efektivní odstranění volných lipidů.

Další úprava podmínek, které se lišily v teplotách a časech saponifikace, ukázala, že prodloužení času saponifikace zlepšilo extrakci ceramidů OS a OdS. Zejména delší doby saponifikace zlepšily výtěžnost ceramidu OS, zatímco vysoké teploty nepříznivě ovlivnily stabilitu volných lipidů a některých ceramidů.

Tato studie identifikovala klíčovou roli teploty a časů čištění/saponifikace v optimalizaci extrakce ceramidů. Nižší teploty a prodloužené doby čištění a saponifikace výrazně zlepšily výtěžnost ceramidů typu OS, OdS a OP, zatímco vysoké teploty vedly k degradaci. Optimalizované postupy uvedené v této studii poskytují spolehlivou metodu pro izolaci a analýzu ceramidů, což nabízí vhled do jejich distribuce a potenciální důsledky pro výzkum zdraví pokožky.

Klíčová slova: Ceramidy, Sfingolipidy, *Stratum corneum*, Lipidová obálka, Kovalentně vázané lipidy, Extrakce lipidů, Saponifikace, Kožní bariéra, Kvantifikace lipidů, Teplotní vliv na lipidy, Výzkum zdraví pokožky.

Table of Contents

1 INTRODUCTION AND AIMS OF THE STUDY

The primary aim of this study was to develop and optimize a reliable procedure for the isolation of covalently bound lipids from human skin samples. Covalently bound lipids, such as Ceramides (Cer), are critical components of the skin's barrier function, playing a significant role in maintaining skin hydration and protecting against external pathogens. Despite their importance, the extraction and analysis of these lipids present a considerable challenge due to their strong association with the protein matrix of the stratum corneum (SC). This study, therefore, sought to address these challenges by systematically investigating the effects of various experimental conditions, including temperature, solvent concentration, reaction time, and extraction methods, on the isolation and quantification of these lipids.

To achieve this goal, the study was divided into a series of experiments, each designed to test and refine specific steps in the lipid extraction process. The approach was highly iterative, with each experiment building upon the findings of the previous one, allowing for the identification of optimal conditions for lipid isolation. The ultimate objective was not only to enhance the efficiency of lipid recovery but also to ensure the preservation of the integrity of these lipids throughout the extraction process. This was crucial for accurate lipid quantification using advanced analytical techniques like liquid chromatography-mass spectrometry (LC-MS^2).

By optimizing the procedures for lipid extraction and analysis, this study aimed to contribute to a deeper understanding of the composition and role of covalently bound lipids in the skin barrier. Such insights could potentially enhance the development of novel therapeutic strategies for skin conditions associated with impaired barrier function, such as atopic dermatitis (AD) and psoriasis.

2 GENERAL OVERVIEW

One of the skin's primary roles is to establish a permeability barrier, commonly known as the skin barrier, which serves to safeguard against the infiltration of external pathogens, allergens, and chemical substances. Simultaneously, it also prevents the body from losing water and electrolytes [1-4]. Diminished skin barrier function raises the susceptibility to, or is a contributing factor in the development of, infectious diseases, psoriasis [5], AD [6], etc.

2.1 Structure of human skin

The skin comprises two primary layers: the epidermis and the dermis. The epidermis is composed of a specialized type of stratified squamous epithelium, with its primary cellular component being the keratinocyte. Keratinocytes are responsible for synthesizing keratin, a structural protein consisting of coiled polypeptide chains that form supercoils through the linkage of several polypeptides via disulfide bonds between neighboring cysteine amino acids. Additionally, keratinocytes produce cytokines when responding to injuries.

The epidermis can be subdivided into four layers [Figure 1]:

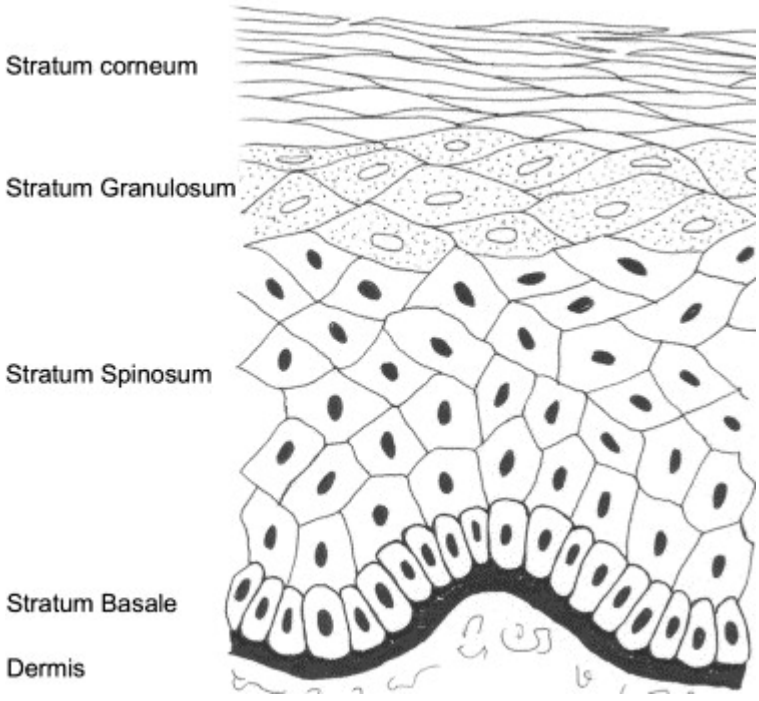

Figure1. Epidermis layers [7]

1. Stratum basale: This bottom layer contains mainly keratinocytes, which can be dividing or non-dividing. Melanocytes, comprising 5-10% of cells, are also present. In some areas, like glabrous skin, it may be two to three cells thick.

2. Stratum spinosum: Basal cells migrate upwards, forming polyhedral cells connected by desmosomes, giving rise to the "prickles" observed under a microscope. Langerhans cells are identifiable within this layer.

3. Stratum granulosum: Keratinocytes in this layer contain granules of keratohyalin and smaller lamellated granules. Lipid discharge between cells contributes to barrier function and cohesion within the SC.

4. Stratum corneum: The outermost layer, composed of flattened corneocytes (terminally differentiated keratinocytes) lacking nuclei and organelles. Keratin filaments align into disulfide cross-linked macrofibres. The thickness varies, with additional zones like the stratum lucidum present in palmoplantar skin. Cell turnover from division to shedding takes about 28 days, modifiable by certain diseases [8].

The human SC is often depicted using various models. The most common model is called the Bricks and Mortar model, where corneocytes are surrounded by a lipid matrix. This lipid matrix adopts specific lamellar and lateral organizations [figure 2], which will be described in more detail below.

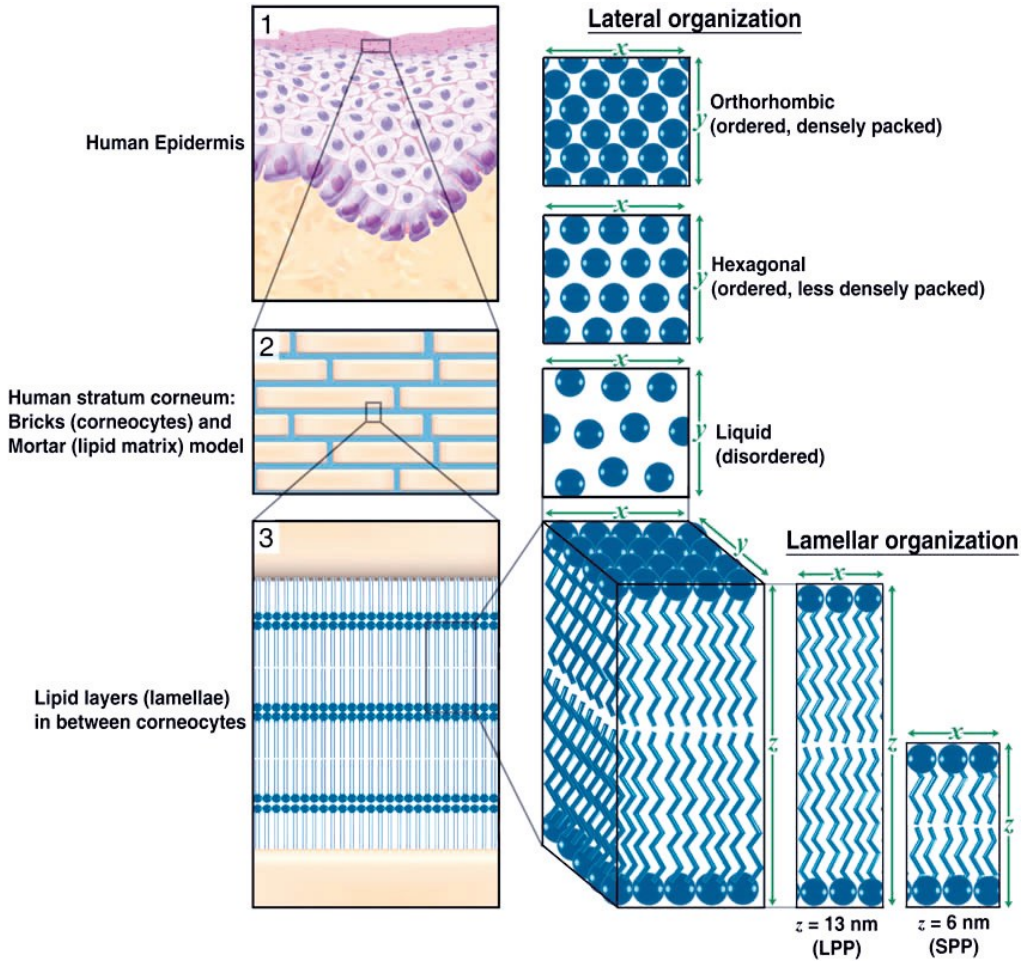

Figure 2. Lamellar and lateral organization in human stratum corneum. (1) The outermost layer of the epidermis, the SC, consists of dead cells (corneocytes) embedded in a lipid matrix, also referred to as the brick (corneocytes) and mortar (lipids) structure (2). The intercellular lipids are arranged in layers (lamellae) (3), with two coexisting lamellar phases. There are three possible lateral arrangements of the lipids: a very dense, ordered orthorhombic organization; a less dense, ordered hexagonal organization; and a disordered liquid organization [2]

1. Brick and Mortar Structure: The outermost layer of the epidermis, known as the SC, is often described as a “brick and mortar” structure. The “bricks” represent terminally differentiated keratinocytes, mainly composed of keratin filaments and filaggrin. The “mortar” consists of intercellular lipids arranged into lamellar layers. These lamellar layers contain Cers, free fatty acids, and cholesterol (CHOL), acting as the binding material that holds the “bricks” together [9].
2. Lamellar Organization: The lipid lamellae, which form a multi-layered lipid structure, are fundamental components of the SC and hold a central role in maintaining the integrity of the skin barrier [10].

The lipid lamellae exhibit a lamellar organization, forming distinct phases. These lamellar phases are essential for maintaining skin barrier function and preventing water loss [11]. We recognize the short periodicity phase (SPP) and the long periodicity phase (LPP). The SPP typically has a repeating distance of about 6.4 nm, associated with a compact arrangement of lipid molecules that contributes to the structural integrity of the skin barrier. In contrast, the LPP is characterized by a longer repeating distance of approximately 13.4 nm, playing a crucial role in the skin's barrier function by allowing for the proper organization and fluidity necessary for effective permeability and protection against environmental factors [12, 13]. Acylceramides (AcylCer) are essential for the formation of the LPP due to their unique structure containing an ultralong acyl chain further esterified by another fatty acid [12, 14].

The study of these lamellar phases is primarily conducted using advanced techniques such as X-ray diffraction, which analyses the periodicity and organization of the lipid layers, providing information on the spacing between adjacent lipid layers and allowing researchers to identify the distinct phases based on their characteristic diffraction patterns [13]. Additionally, transmission electron microscopy is employed to visualize the lamellar structures at high resolution, with staining techniques helping to distinguish between lipid headgroups and hydrophobic tails, thereby revealing the layered organization of the membranes.

3. Lateral Organization: The lipids within the lamellar layers are also organized laterally. In healthy human SC and the presence of Cers, CHOL and FFAs, the lipids adopt mostly an orthorhombic packing pattern. This lateral organization ensures the stability and functionality of the skin barrier [12].

   However, in several skin diseases with impaired barrier function, such as AD, lamellar ichthyosis, Netherton syndrome (NS), and psoriasis, a higher fraction of lipids adopts a hexagonal lateral packing compared to healthy skin. The hexagonal packing is less ordered and dense than the orthorhombic packing found in healthy SC [15]. Fourier-transform infrared spectroscopy is also utilized to assess the lipid

composition and interactions between different lipid classes, further elucidating the structural characteristics of the lamellar phases [14][figure 3].

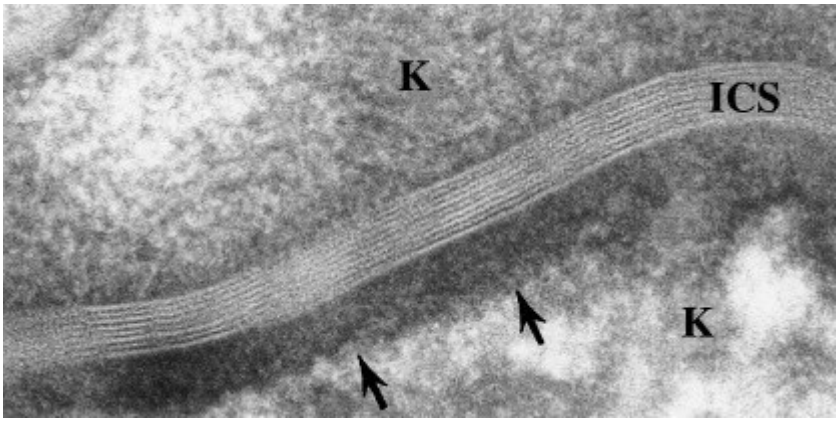

Figure 3. Electron micrograph showing the stacked and patterned lamellar membrane sheets in a single intercellular space in mouse SC postfixed with ruthenium tetroxide. ICS, intercellular space; K, keratin contents of the corneocytes bordering the intercellular space [16]

2.2 Diversity and Function of Ceramides in the human Stratum corneum

2.2.1 Implications for Skin Health

Within the human SC, various Cer species coexist, and a reduction in Cer levels or alterations in Cer composition are closely associated with the occurrence of AD, psoriasis, Ichthyoses, Xerosis and other skin disorders [1, 2, 17, 18].

Cers are composed of a long chain base (LCB) that is connected to a fatty acyl (FA) through an amide bond. Mammals possess five distinct types of LCBs: dihydrosphingosine (DS), sphingosine (S), phytosphingosine (P), 6-hydroxysphingosine (H) and 4,14-sphingadiene (SD). These types of LCBs vary in the number and location of their hydroxyl groups and double bonds [19, 20][Figure 4A].

LCBs can be classified based on the number of hydroxyl groups (d for di/2, t for tri/3), carbon atoms, and double bonds. For instance, in a carbon chain length of 18, five LCB types are represented as follows: d18:0 (DS), d18:1 (S), t18:0 (P), t18:1(6OH) (H), and d18:2 (SD). Additionally, Cer FAs in humans fall into four categories: nonhydroxy, α-hydroxy (A), ω-hydroxy (O), and esterified ω-hydroxy (EO) FAs [19][Figure 4B]. Figure 3B also shows a β-hydroxy FA, but in human skin, it could be found in very minor

quantities. EO-type Cers known as AcylCers, primarily have linoleic acid (LA) attached to their ω-position [21].

Human Cers are categorized into 20 classes based on their combination of LCB and FA. Each Cer class is identified using abbreviations for its specific type of FA and LCB. For instance, a Cer class made up of a nonhydroxy FA (N) and S is represented as Cer NS [22]. Additionally, the SC contains both free Cers forming the lipid lamellae in extracellular space and also protein-bound Cers. These protein-bound Cers, known as P-O-type Cers, are covalently attached to the surface proteins (cornified envelope proteins) of corneocytes forming a so-called corneocyte lipid envelope (CLE) [23-26][Figure 3] [Figure 4C].

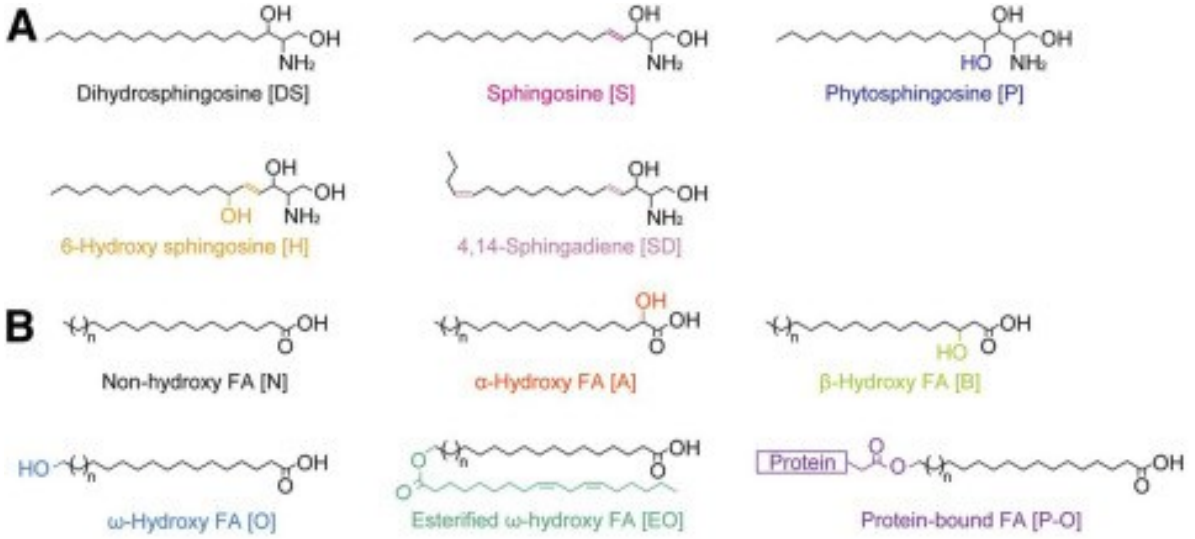

C

FAs \ LCBs	Dihydro-sphingosine [DS]	Sphingosine [S]	Phytosphingosine [P]	6-Hydroxy sphingosine [H]	4,14-Sphingadiene [SD]
Non-hydroxy [N]	NDS	NS	NP	NH	NSD
α-Hydroxy [A]	ADS	AS	AP	AH	ASD
β-Hydroxy [B]	BDS	BS	BP	BH	BSD
ω-Hydroxy [O]	ODS	OS	OP	OH	OSD
Esterified ω-hydroxy [EO]	EODS	EOS	EOP	EOH	EOSD
Protein-bound [P-O]	P-ODS	P-OS	P-OP	P-OH	P-OSD

Figure 4. Structures and nomenclature of human ceramide classes: A, B: Structures of LCBs (A) and FAs (B) in human ceramides. C: Notation of ceramide classes involves a combination of abbreviations for types of FA and LCB. Each ceramide class is represented by abbreviations denoting its specific FA and LCB types [27]

2.2.2 Key Roles of Ceramides in Skin Barrier Formation

Cers serve as the hydrophobic core structure within sphingolipids, a prominent lipid group found in cell membranes. In most tissues, Cer levels remain low because they are transiently produced during the synthesis and breakdown of sphingolipids. Additionally, in most mammalian tissues, only a limited variety of Cer classes are present; the dominant class consists of N combined with S, while other classes are found in minimal quantities or are restricted to specific tissues [27]. In contrast, the SC contains abundant levels of Cers belonging to multiple classes, allowing it to fulfil its specialized function, particularly in maintaining the skin barrier [28]. The chain length of Cers can vary, and this variation is significant because it has been found that some functions of Cers are chain-length dependent [29]. Cers are central molecules in the metabolism of sphingolipids and serve as precursors for the biosynthesis of complex sphingolipids like glucosyl Cers, sphingomyelins, gangliosides, etc. They affect the regulation of cells such as growth, metabolism, differentiation, and death, also in SC extracellular space, they help maintaining the epidermal water barrier. The length of the acyl chain in Cers varies mostly from 14 to 24 carbons (N and A subclasses) and between 28 – 36 carbons (EO and O subclasses). In some tissues, there are also ultra-long Cers with differing structures (male germ cells ≥30 C) [30].

Free fatty acid (FFA) consists of a single hydrocarbon chain, whereas Cers have two hydrocarbon chains, and these two lipid types vary in their molecular structures: FFAs are mainly saturated, whereas Cers consist of a sphingoid base linked to a FA chain. Both FFAs and Cers exhibit a diverse range of carbon chain lengths [10].

2.3 Biosynthesis

2.3.1 Cer Generation

The biosynthesis of sphingolipids is a complex process that primarily takes place in the endoplasmic reticulum beginning with the de novo synthesis of Cers from non-sphingolipid precursors [31, 32]. The sphingoid base synthesis process begins with the condensation of L-serine and palmitoyl-CoA, facilitated by the enzyme serine palmitoyltransferase, to generate 3-ketodihydrosphingosine.

The 3- ketodihydrosphingosine is reduced to DS by the enzyme 3- ketodihydrosphingosine reductase. The DS is then acylated by Cer synthases to form dihydroceramide. In mammals, there are six Cer synthases (CerS1-6), each of which shows a preference for different lengths of fatty acid chains, resulting in Cers with different acyl chain lengths [33]. Dihydroceramide is then subsequently desaturated by desaturase 1 to form Cer or by desaturase 2 to form phytoceramide [34]. This process is tightly regulated and compartmentalized within the cell [Figure 5].

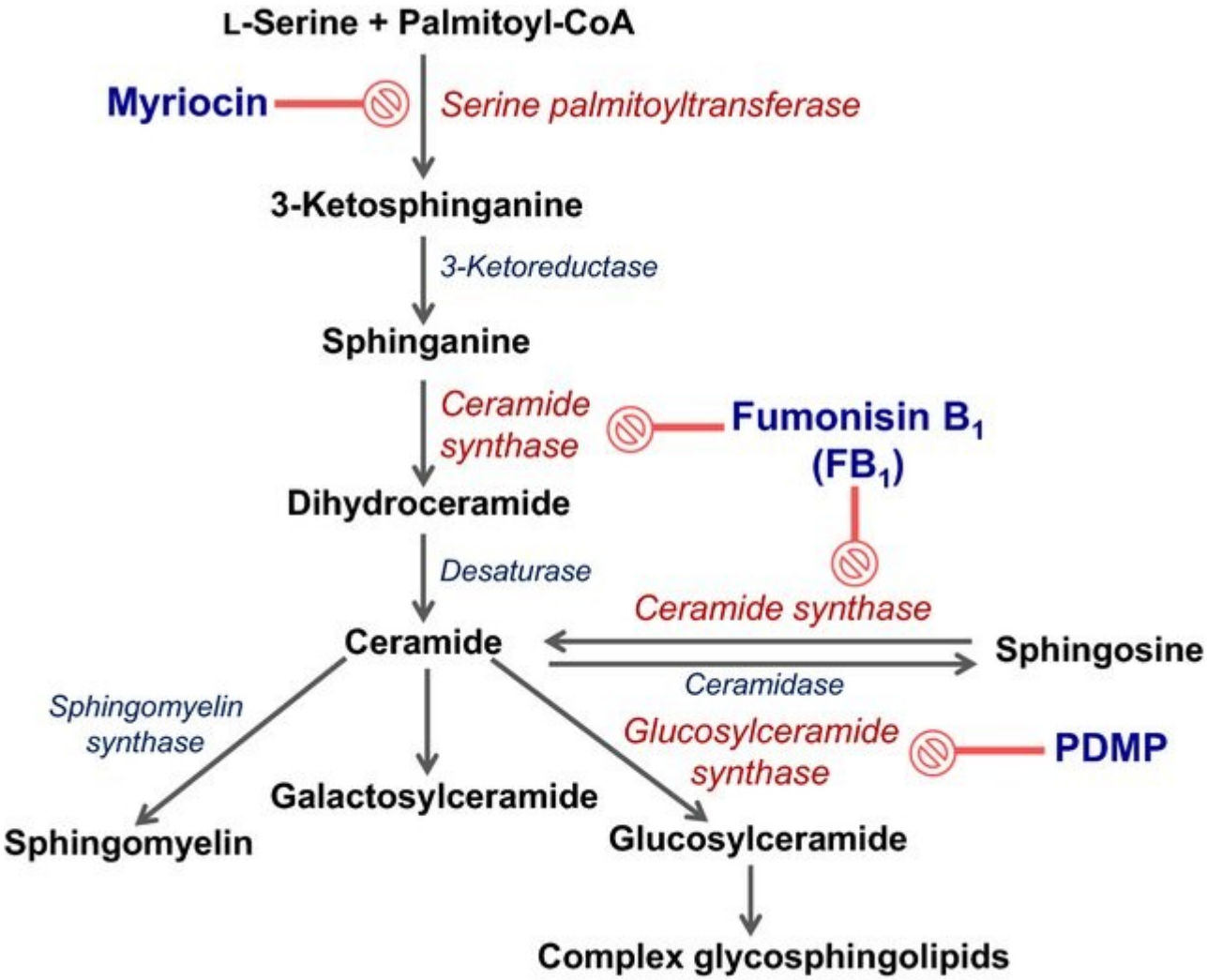

Figure 5. Metabolic pathway for sphingolipid biosynthesis and commonly used inhibitors in various stages of the pathway [35]

2.3.2 Ceramide Transport to the Stratum Corneum

Since Cers are highly lipophilic and not very well suitable for direct transport, the newly synthesized Cers are converted into glycosphingolipids (GlcCer) and sphingomyelin (SM) within the Golgi apparatus. The synthesis of GlcCer is carried out by the enzyme

GlcCer synthase, primarily on the cytosolic face of the cis/medial Golgi. Once synthesized, GlcCer can be progressively glycosylated to form complex glycosphingolipids in the distal Golgi. This process is part of the metabolic pathways involved in the synthesis and metabolism of Cers and other sphingolipids [36].

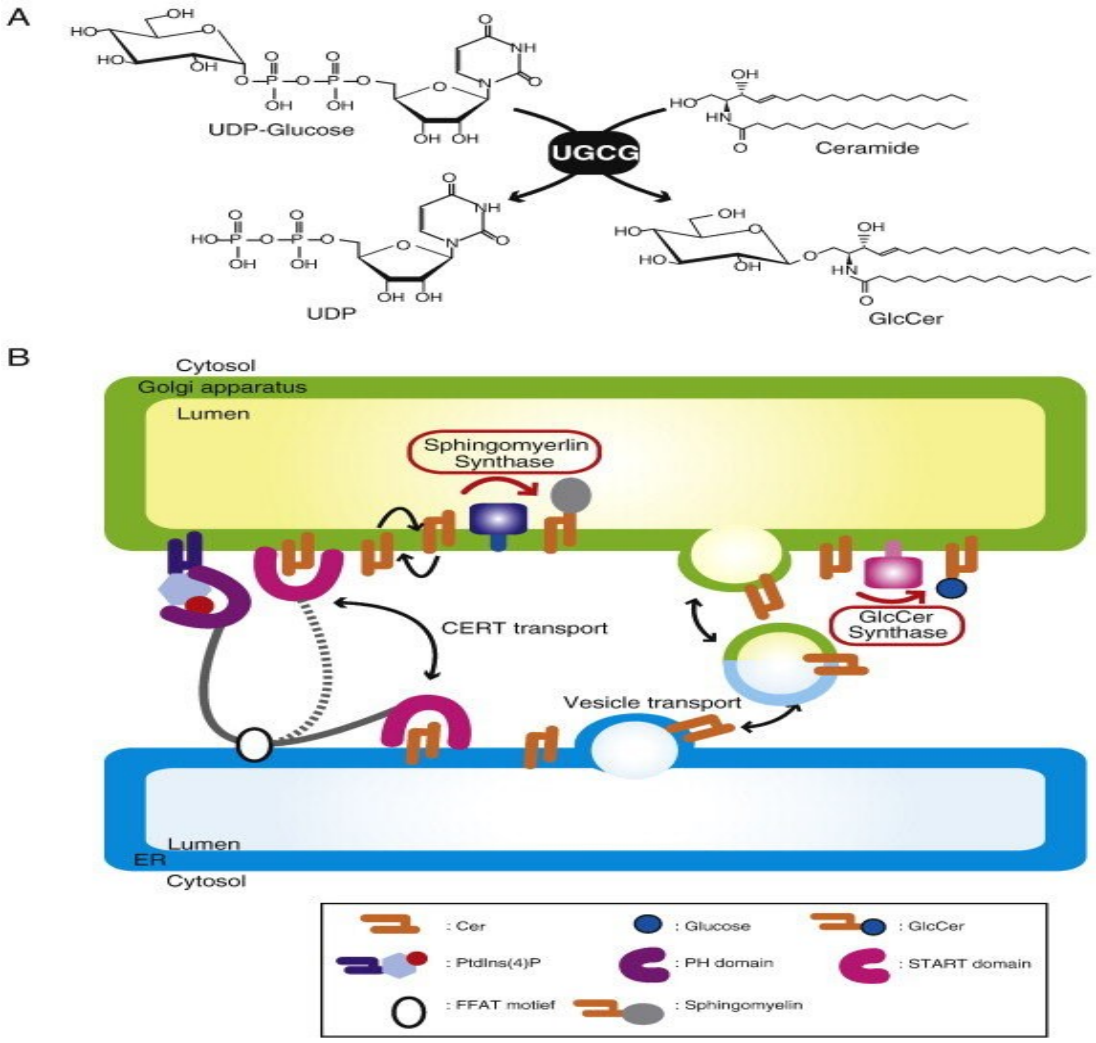

Figure 6. Machinery of GlcCer synthesis. (A) The reaction scheme of GlcCer synthesis was catalyzed by UGCG. (B) Ceramide transport pathways are involved in the synthesis of GlcCer and sphingomyelin [37]

SMs are synthesized at two locations: the inner trans-Golgi and the plasma membrane, facilitated by two distinct SM synthase isoforms. After synthesis, GlcCer and SM are packaged into lamellar bodies and secreted at the stratum granulosum-stratum corneum interface. Here, they undergo hydrolysis back to Cer species. Sphingomyelinase and glucocerebrosidase [38-40] convert SM and GlcCers into Cers, respectively [36][Figure 6].

2.3.3 AcylCeramide Generation

2.3.3.1 VLFA synthesis

FA with carbon chain lengths up to C16 is synthesized by the FA synthase complex in mammals [41]. Afterward, the membrane-linked fatty acid chain elongation system synthesizes very long-chain fatty acids with a chain length of C18 or greater than C16 fatty acids [41] [Figure 7]. Both the initial fatty acid synthase complex and the fatty acid chain-elongation system utilize four enzymatic steps for chain elongation: condensation catalyzed by 3-ketoacyl CoA synthase, reduction by 3-ketoacyl CoA reductase, dehydration by 3-hydroxyacyl CoA hydratase, and another reduction step by 2,3 enoyl CoA reductase [41]. Each cycle of this process adds two carbon atoms to the chain. In yeast, Elo1p, Elo2p, and Elo3p are known to catalyze condensation, while in mammals, six ELO homologs (ELOVL1–6) have been identified. ELOVL1, with broad substrate specificity up to C24, along with ELOVL3 (C22–26) and ELOVL6 (C12–16–18), are involved in elongating both saturated and monounsaturated very long-chain fatty acid synthesis [41]. ELOVL2 (C16–20), ELOVL4 (C20, 22), and ELOVL5 (C16–20) are implicated in elongating polyunsaturated fatty acids.

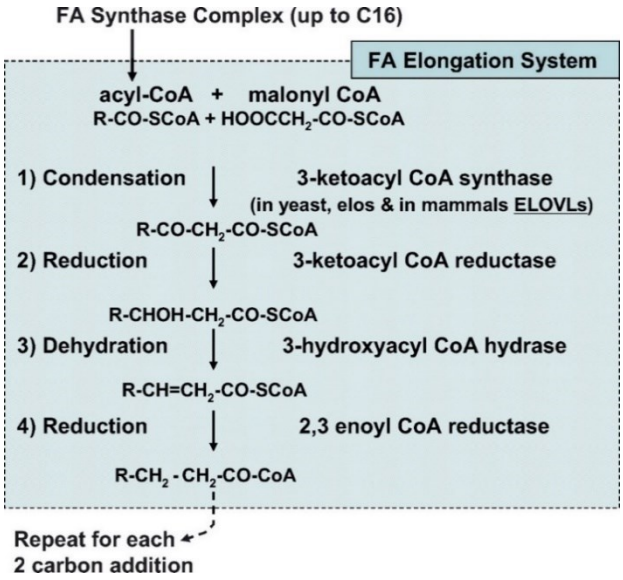

Figure 7. The elongation process synthesizes very long-chain fatty acids with a chain length equal to or greater than C18 through the membrane-associated fatty acid chain-elongation system [41]

However, the specificities of substrates and products for ELOVLs remain incompletely understood. Although ELOVL1 is expressed widely across mammalian tissues, other ELOVLs exhibit tissue-specific expression patterns [41]. In the AcylCer biosynthesis,

the most important elongase is the ELOVL4, which is the only one able to elongate chains over 28 carbons. The loss of ELOVL4-generated VLFA and ω-O-AcylCers is likely the underlying cause of the early mortality observed in mice with the homozygous 5 bp-deletion mutation [42].

2.3.3.2 Completion of the AcylCeramide molecule

The first step in AcylCer biosynthesis involves the ω-hydroxylation of ultra-long-chain fatty acids by the cytochrome P450 enzyme CYP4F22. This enzyme is essential for the synthesis of AcylCer, which plays a crucial role in skin barrier formation. Mutations in CYP4F22 have been linked to skin disorders such as lamellar ichthyosis, highlighting its importance in lipid metabolism and epidermal health [43, 44].

Next, the attachment of the ω-hydroxylated fatty acid to sphingosine is catalyzed by Cer synthase 3 (CerS3). CerS3 facilitates the formation of Cers by linking sphingosine with fatty acids with a chain longer than C28, including the ω-hydroxylated ultra-long-chain fatty acids [43-45].

The final step involves the incorporation of LA into the AcylCer molecule, which is catalyzed by the enzyme PNPLA1. This enzyme is responsible for attaching LA to the ω-hydroxyl group of the Cer, completing the AcylCer structure. The presence of LA is crucial for the structural and functional properties of AcylCer in the skin barrier [43, 46, 47].

Linoleic acid, an essential fatty acid (EFA), is crucial for maintaining the skin's permeability barrier, and its deficiency can lead to significant dermatological issues. It was claimed that LA plays a direct role in barrier function, demonstrating that inadequate levels of this fatty acid compromise the integrity of the skin barrier, resulting in increased transepidermal water loss and dryness. When the levels of LA in a diet are low, other acids like oleic or stearic are used for the biosynthesis of the AcylCer. It leads to essential fatty acid deficiency (EFAD) which is characterized by clinical manifestations such as scaly dermatitis and hair loss, which arise from disrupted Cer synthesis, as LA is a key component in the formation of these lipids. Biochemical markers of EFAD, including elevated Mead acid levels and reduced linoleic and arachidonic acid levels, provide evidence of impaired fatty acid metabolism. Consequently, dietary recommendations

suggest that at least 2-4% of total caloric intake should be derived from LA to support skin health and prevent the adverse effects associated with its deficiency. Thus, ensuring adequate LA intake is essential for maintaining skin barrier function and overall dermatological health [48]. EFAD can be effectively treated with sufficient amounts of EFAs. It was indicated that oral preparations containing EFAs may alleviate EFAD symptoms [49, 50].

After the AcylCer completion, the AcylCer is glucosylated at the Golgi apparatus using UDP-activated glucose [51]. This glucosylation step is essential for the processing of AcylCers into the extracellular lipid lamellae that form the skin's permeability barrier [52]. The glucosylated AcylCers are then secreted from the keratinocytes and transported to the SC. Finally, the glucose moiety is cleaved off, likely by β-glucocerebrosidase, leaving the mature AcylCer molecule in the extracellular space [53, 54].

2.3.4 AcylCeramide oxidation and attachment to the corneocyte envelope

It is proposed that the chemical reactivity of the epoxy-enone with protein is key to the role of the enzymatic pathway in forming the CLE. 12*R*-lipoxygenase (12*R*-LOX) and epidermal lipoxygenase-3 (eLOX3) are key enzymes involved in the oxidation of linoleic acid, particularly in the context of skin barrier function [55]. 12*R*-LOX catalyzes the initial oxidation of LA when it is esterified in Cers within the epidermis, generating a 9*R*-hydroperoxide of linoleic acid. This step is crucial for the formation of bioactive lipid mediators that contribute to the skin's barrier properties, helping to maintain skin hydration and integrity [26, 56]. Following this, eLOX3 acts on the oxidized products of linoleic acid, isomerizing the 9*R*-hydroperoxide produced by 12*R*-LOX into epoxy derivatives [57]. The last enzyme in this oxidation pathway is SDR9C7, which facilitates the formation of CerEOS-epoxy-enone. Figure 8A illustrates the normal oxidative pathway, while Figure 8B shows the alterations when SDR9C7 is blocked or absent. LC-MS^2 analysis of the oxidized Cers has established that loss of SDR9C7 results in the accumulation of pathway precursors (CerEOS, CerEOS-9-HODE, CerEOS-epoxy-alcohol) and a significant buildup of CerEOS-triol as a bypass route.

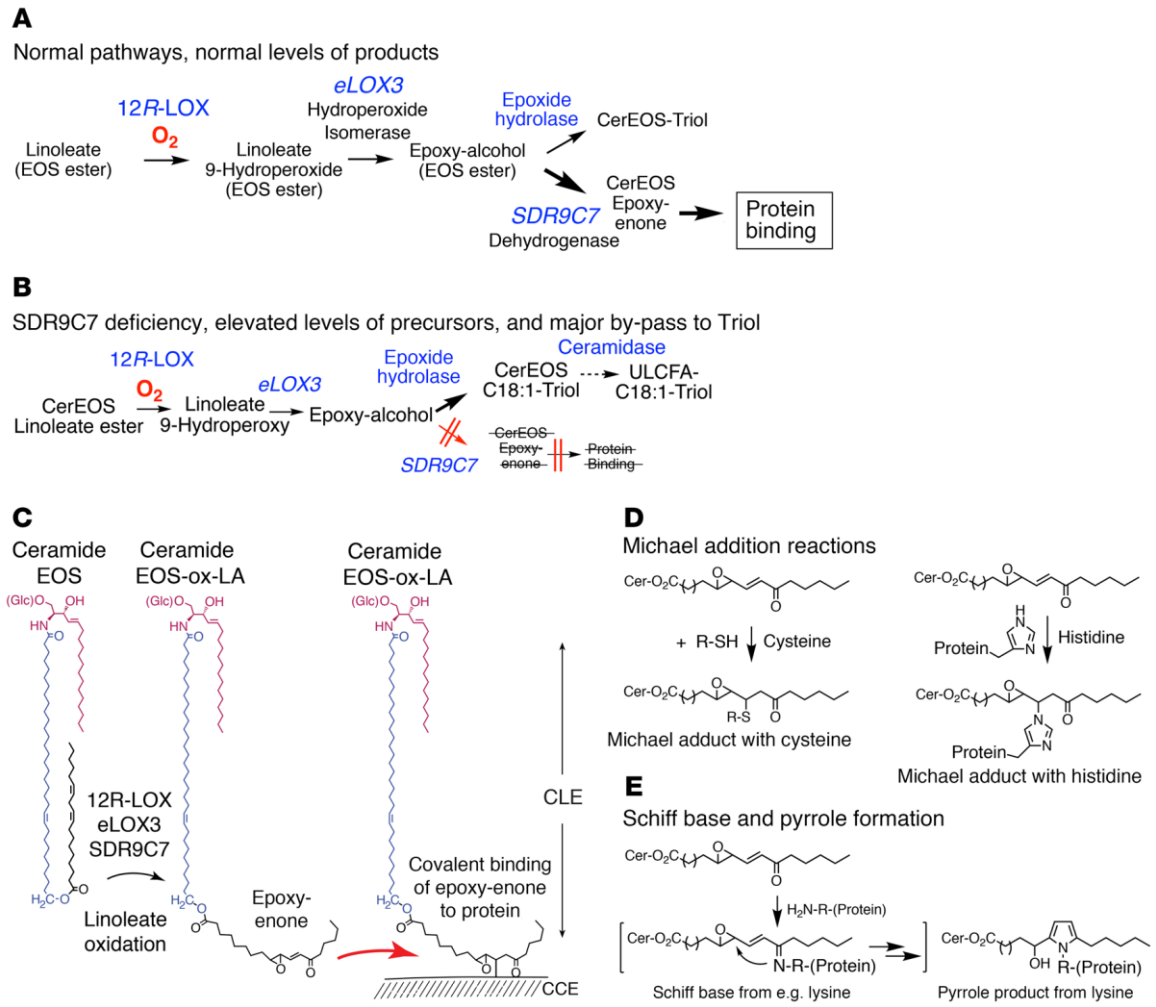

Figure 8. Potential modes of protein binding by covalent reactions of EOS-epoxy-enone [58]

The formation and function of the CLE during epidermal terminal differentiation have long been enigmatic. Recent insights from research into inherited and acquired disorders of lipid metabolism shed new light on this critical structure. A new hypothesis suggests that CerEOS-epoxy-enone, generated by the SDR9C7-mediated transformation, facilitates Cer binding to cornified cell envelope (CCE), initiating CLE formation [Figure 8C]. The epoxy-enone moiety's chemical reactivity has been supported by literature for its role in protein binding. It is proposed that the α/β-unsaturated ketone reacts with cysteine, histidine, and lysine residues via Michael addition [Figure 8D] or that fatty acid attachment to proteins occurs through Schiff base formation with amino groups [Figure 8E]. Although these reactions are reversible, they may promote close ceramide-protein association, leading to irreversible binding [59-61].

2.3.5 Ceramide degradation pathways

2.3.5.1 Conversion to Acyl-CoA

In Cer degradation pathways, it is the Ceramide fatty acyl chain that is cleaved and then converted into acyl-CoA. This conversion is facilitated by acyl-CoA synthetases, which are vital for incorporating fatty acids into lipids and generating lipid mediators such as sphingosine 1-phosphate (S1P). This pathway plays a significant role in sphingolipid metabolism, allowing for the integration of Cer-derived components into glycerophospholipids and other lipid species [19].

The decomposition of S1P is the only pathway leading to the complete degradation of sphingolipids. Specifically, S1P can be irreversibly degraded by S1P lyase into phosphoethanolamine and hexadecenal, which is described as the final degradation step of sphingolipid species [62].

2.3.5.2 Hydrolysis and Salvage Pathway

The salvage pathway, also known as sphingosine recycling, involves the enzymatic hydrolysis of GlcCer and SM to Cer. Cer can then be further hydrolyzed by ceramidases into sphingoid bases and fatty acids. This pathway is crucial for recycling sphingolipid components, enabling the re-utilization of sphingolipids as substrates for Cer formation. For example, Cer can be converted back into sphingosine and non-hydroxy fatty acids, which can subsequently be re-acylated to produce various Cer species, including Cer 1, Cer 2, and Cer 5 [19, 63][Figure 9].

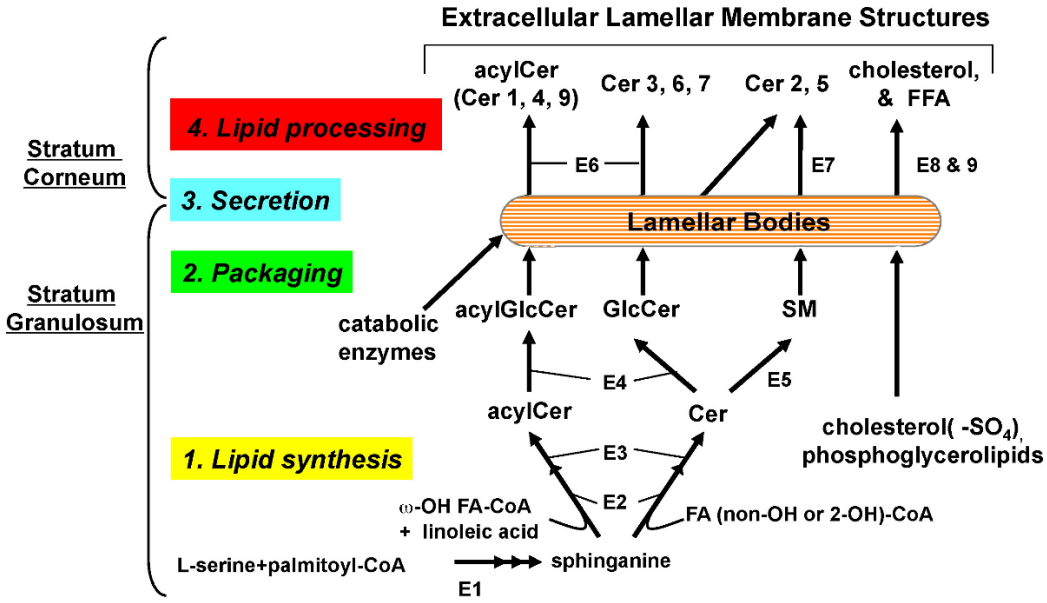

Figure 9. The formation of epidermal barrier lipids involves four main steps that occur during keratinocyte differentiation: (1) Lipid generation is increased, (2) These lipids and their precursors are packaged into epidermal LB, (3) The LB contents are secreted into extracellular domains during the transition from the stratum granulosum to the SC, (4) The secreted lipids are then converted into their hydrophobic counterparts. These steps result in the formation of extracellular lamellar membrane structures in the SC, which are crucial for epidermal permeability [64]

2.3.5.1 Enzymatic Transformations

After the initial *N*-acylation step in Cer synthesis, the sphinganine portion of the Cer molecule can undergo further transformations. It can be desaturated to form sphingosine (also known as sphinganine) through the action of desaturase-1 (DES1) or hydroxylated to produce 4-OH sphinganine (phytosphingosine) by desaturase DES2 or to 6-OH sphingosine by unidentified enzymes. These transformations are integral to the diversity of Cer species and their biological functions [19].

2.3.5.2 Molecular Remodeling

The salvage pathway also facilitates the molecular remodeling of pre-formed Cer molecules. This process allows for the modification of Cer structures, which can enhance their functional roles within cellular membranes and signaling pathways. The ability to convert Cer into various sphingolipid forms underscores the dynamic nature of sphingolipid metabolism [19].

2.4 Skin disorders connected with lipid composition and organization

When examining diseased skin, it often exhibits a compromised barrier function. To investigate whether alterations in the properties of lipids in the SC contribute to this impaired skin barrier, it's crucial to gather information on lipid composition and organization. Even if lipid properties are not the primary cause of the disease, such studies can offer valuable insights into the mechanisms underlying changes in lipid composition and, consequently, lipid organization. These insights may provide clues about how lipid properties relate to changes in factors like skin barrier protein expression, the proliferation and differentiation of keratinocytes, or the presence of inflammation [10]. Because variations in SC lipid properties are expected to be much more pronounced in diseased skin (which has a compromised skin barrier function) compared to healthy skin, it becomes easier to establish correlations between lipid composition, lipid organization, and skin barrier function.

2.4.1 Ichthyosis

Ichthyoses is a group of genetic skin disorders characterized by dry, thickened, scaly skin. There are over 20 types of ichthyosis that vary in severity, appearance, genetic cause, and mode of inheritance [65, 66].

2.4.1.1 Ichthyosis vulgaris (IV):

The mildest and most common form, accounting for over 95% of cases. Symptoms appear around 3 months of age as patches on the palms and soles that gradually spread to the rest of the body. It is caused by mutations in the FLG gene that encodes filaggrin, a protein important for skin barrier function [67, 68]. Genetic linkage analyses in IV families mapped the FLG gene to the epidermal differentiation complex on chromosome 1q21 [69, 70]. Genotyping revealed that loss-of-function mutations in the FLG gene cause IV [71], which is inherited in a semi-dominant manner with 83–96% penetrance [72-74]. Mutations lead to a truncated profilaggrin protein that cannot be processed into functional filaggrin subunits [75]. It is still possible that mutations in related genes could also result in truncated filaggrin proteins [76, 77].

2.4.1.2 X-linked ichthyosis:

In the early 20th century, an ichthyosis subtype inherited as an X-linked recessive trait (i.e., transmitted from unaffected female carriers to sons) was identified [78]. Biochemical studies in skin fibroblasts of affected individuals correctly predicted a deficiency in the enzyme steroid sulfatase (STS) as a causal mechanism [79] and the STS gene was subsequently cloned [80]. STS cleaves sulfate groups from multiple steroid hormones (e.g., dehydroepiandrosterone sulfate, DHEAS), affecting their water solubility, bioavailability, and activity [81]. The central mechanism behind the skin phenotype in X-linked recessive ichthyosis is probably an accumulation of CHOL sulfate (and a deficit of CHOL) in the SC [82, 83].

2.4.1.3 Autosomal recessive congenital ichthyosis:

Autosomal recessive congenital ichthyosis (ARCI) is a heterogeneous group of monogenic genodermatoses characterized by disorders of keratinization that lead to significant skin barrier dysfunction. Patients with ARCI often exhibit a disturbance in epidermal lipid metabolism, which impairs the function of the SC and results in permeability barrier defects. Recent studies have identified defects in the PNPLA1 gene as a significant cause of ARCI. Mutations in PNPLA1 disrupt the synthesis of ω-*O*-AcylCers, essential lipids for maintaining the skin's permeability barrier. Functional characterization of PNPLA1 has shown that it acts as a transacylase, transferring LA to ω-hydroxy fatty acids in Cer, thereby producing ω-*O*-AcylCers. In patients with ARCI, novel mutations in PNPLA1 have been linked to severe epidermal permeability defects, leading to an accumulation of Cer precursors and a near-total absence of ω-*O*-AcylCers in the SC. This deficiency contributes to the disorganization of the extracellular lipid matrix and the cornified lipid envelope, which are critical for skin barrier integrity. Additionally, knockout mouse models lacking PNPLA1 exhibit similar skin permeability issues, further supporting the irreplaceable function of PNPLA1 in epidermal ω-*O*-AcylCer synthesis and skin barrier maintenance [47].

It includes subtypes like lamellar ichthyosis and harlequin ichthyosis. Harlequin ichthyosis is the most severe, with a collodion membrane at birth that later forms large, thick, ridged scales [84].

Lamellar ichthyosis was among the first skin diseases where comprehensive information about both the lipid composition and organization in the SC was acquired [85, 86]. Patients with this condition exhibited a compromised skin barrier function, as evidenced by a significant increase in transepidermal water loss (TEWL). Regarding the lipids, there was a notable decrease in the ratios of FFA to CHOL and FFA to Cers, while the Cer to CHOL ratio remained similar to that in healthy skin. These findings suggest a substantial reduction in the FFA levels within the lipid matrix of the SC [87]. In addition to these alterations in lipid composition, individuals with lamellar ichthyosis also displayed changes in the organization of their lamellar lipids [88].

2.4.1.4 Netherton syndrome:

NS is an autosomal recessive disorder characterized by congenital ichthyosiform erythroderma, trichorrhexis invaginata (Bamboo hair), and atopic diathesis. Affected children present with generalized ichthyosiform erythroderma at birth, which may persist or evolve into ichthyosis linearis circumflexa, marked by serpiginous, migratory erythematous patches with double-edged scales. Children with NTS often experience severe growth and developmental delays due to diarrhea, intestinal malabsorption, recurrent infections, and hypernatremic dehydration. The pathognomonic sign of NTS, trichorrhexis invaginata, can be diagnosed through hair dermatoscopy, revealing brittle hair and poor growth [89]. In NS, significant alterations in SC lipids are observed, including decreased FFA chain length and increased levels of monounsaturated FFAs, alongside a notable rise in short-chain Cers and a reduction in long-chain Cers. These lipid composition changes lead to disordered lipid organization, contributing to the impaired skin barrier function characteristic of the condition [10].

2.4.1.5 Acquired ichthyosis:

Acquired ichthyosis (AI) is an extremely rare, nonhereditary cutaneous disorder which is characterized by prominent fish-like scaling, hyperkeratosis, and a reduced or absent granular layer in histology. Management includes topical treatments and, in more severe cases, systemic therapies [90]. AI, typically presenting in adulthood, has been linked to various conditions, including neoplastic, infectious, drug-related, endocrine, metabolic, autoimmune, and malabsorptive diseases [91, 92].

2.4.2 Psoriasis

It is another skin condition in which the role of lipids has been explored concerning skin barrier function. Psoriasis is a chronic inflammatory skin disease that affects approximately 2% of the population in Western countries. Research into the genetics of psoriasis suggests that epidermal immunology plays a role in the condition [93, 94]. However, it's also possible that the disease results from primary abnormalities in skin barrier functions [95, 96]. Psoriasis is characterized by abnormal epidermal cell proliferation, which leads to incomplete differentiation. Analyses conducted on patients with psoriasis demonstrated a significant decrease in skin barrier function. This was evident through increased TEWL values observed on psoriatic plaques and fissured areas of the skin, while the increase in TEWL was not significant in unaffected skin. In psoriasis, the depletion of SC lipids, especially Cers, is localized to the lesional epidermis and directly correlates with the severity of the skin condition [10, 97]. Psoriasis is associated with altered expression of epidermal lipid biosynthesis enzymes and changes in SC lipid composition [98].

2.4.3 Atopic dermatitis

When it comes to the investigation of lipid composition and organization, it stands out as one of the most extensively studied skin conditions. AD is a chronic and recurring inflammatory skin disorder characterized by a wide range of clinical symptoms, including erythema (redness), dryness, and severe itching (pruritus) [99, 100]. Patients with AD exhibit reduced skin barrier function in both affected (lesional) and unaffected (non-lesional) skin [101-105]. While mutations in the FLG gene are currently recognized as the primary genetic risk factor for the development of AD [68, 106-110], it's crucial to acknowledge that this complex skin condition is influenced by a range of other factors, including immunological and environmental elements [99, 111-113]. In patients afflicted with AD, the intricate balance of Cer composition within the skin's barrier is disrupted, as revealed through comprehensive immunofluorescence analyses. CerS3 exhibited distinct expression patterns in both control and AD non-lesional skin, manifesting as a singular cell layer band along the stratum granulosum, with attenuated expression in deeper epidermal layers. Similarly, acid sphingomyelinase, pivotal in Cer synthesis

pathways, displayed a gradient expression profile in control and non-lesional AD skin, with its highest expression concentrated in the stratum granulosum. Glucocerebrosidase (GBA), another key player in Cer metabolism, exhibited distinct patterns of expression. In control skin, GBA was primarily localized at the stratum granulosum-stratum corneum interface, with minimal staining in deeper layers. However, in AD lesional skin of patients with elevated SCORAD scores (a clinical tool used to assess the severity of AD), GBA expression extended to 2–3 cell layers along the stratum granulosum and stratum spinosum, hinting at altered expression in response to disease severity. These findings underscore significant perturbations in Cer metabolism in AD patients, marked by dysregulated expression of CerS3, aSMase, and GBA, particularly within lesional skin and in tandem with disease severity, unaffected by FLG mutations [114].

In AD skin, there is limited information available regarding the composition of FFAs compared to Cers. However, it has been reported that the levels of very long-chain fatty acids (those with more than 24 carbon atoms) are reduced in both non-lesional and lesional skin of AD patients [115].

In terms of variations in Cer subclasses, deficiencies in enzymes such as β-glucosylceramidase and sphingomyelinase are frequently reported in connection with AD. These enzyme deficiencies can impact the metabolism of Cers and other sphingolipids, potentially contributing to the altered lipid profiles observed in individuals with AD. Such enzyme deficiencies are one aspect of the complex biochemical and genetic factors that may influence the development and progression of AD [116-118].

3 RESULTS AND DISCUSSIONS

This study aimed to develop and optimize procedures for the isolation of covalently bound lipids. To achieve this, the project was systematically divided into seven individual experiments, each focusing on varying specific conditions at particular steps of the process. By methodically altering parameters such as temperature, solvent concentration, reaction time, and extraction methods, we sought to identify the most effective combination of conditions for the successful isolation of these lipids. The following sections detail the outcomes of these experiments and discuss their implications for the overall optimization process.

In general, each procedure was composed of 3 subsequent steps. The first step was always an extraction of free lipids, which separated the extractable lipids from the remaining pellet (containing the covalently bound lipids). The second step was the purification of the pellet to ensure that all the free lipids were removed. The third step was a saponification of the covalently bound lipids (alkaline hydrolysis). After these steps, the isolated lipids which were previously covalently bound, were analysed using LC-MS^2.

The first experiment was conducted from the combination of procedure A of the purification and procedure A of the saponification based on the modified procedure from the article [47]. The details of these procedures are described in the Experimental section, for clarity, the main parameters of individual procedures are summarized in Table 1.

Pellet purification		
Procedure	Temperature and time	Solvent
A	3 x 15 min at 40°C + 2 x 2 h at 60°C	MeOH
B	2 x 3 h at 60°C + 1 x 16 h at 60°C	$CHCl_3$/MeOH 1:2
C	3 x 15 min at 40°C	MeOH
Saponification		
Procedure	Temperature and time	Solvent
A	2 h at 60°C	1M KOH + MeOH
B	1–2 h at 37-50°C	3M KOH + $CHCl_3$/MeOH/H_2O
C	1 h at 60°C	1M KOH + $CHCl_3$/MeOH/H_2O

Table 1. General summary of purification and saponification procedures. Details are described within the individual experiments in the Results and Discussions section and in the Experimental section

According to the procedure, the samples underwent two separate 2-hour incubations in a 60°C bath: the first for the extraction of free lipids using MeOH, and the second for

saponification with a 1M KOH and MeOH solution. As per the results, there were almost no free lipids in the tubes, which was satisfactory as a goal (these free lipids would bias the analysis of the covalently bound lipids); however, due to high temperatures during the pellet purification and saponification, the covalently bound lipids were also entirely damaged; therefore, no covalently bound lipids were detected in the test tubes after LC-MS^2 analysis.

Then we proceeded with the second experiment, which was a combination of procedure B of the purification and procedure C of the saponification, according to the paper [119]This experiment was mainly focused on confirming whether the high temperature during the first experiment caused the damage to the covalently bound lipids or if there was some other issue during that experiment.

The free lipid extraction was performed in the same way as the first experiment. This procedure was previously described in the literature, and we only applied small modifications like a prolongation of the saponification time[119]As per the results, the free lipid extraction was successfully done, and after analysis by LC-MS^2, we observed a decreased presence of covalently bound lipids, raising concerns that the high temperature used in the purification step may have caused lipid damage. Indeed, the majority of these covalently bound lipids were found to be degraded, confirming that the high temperature is responsible for their decomposition.

Then in order to definitively confirm that high temperatures in the incubation of saponified solution is not a good way, we performed the third experiment, which was very similar to the first experiment, but purification was done at 60°C two times for 3 hours and the third time for 16 hours instead of two times for two hours according to the journal paper [120] This experiment combined process B for washing and A for saponification. The results showed that all the free lipids were damaged, and as a consequence of the high temperature, no covalently bound lipids were observed.

After discussions, we decided to continue with the modification of the procedure from the second experiment, and so we did the fourth experiment. From this point, the temperatures for pellet purification and saponification were significantly decreased. Also,

the concentration of KOH increased from 1M in procedure A to 3M KOH in procedure B of the saponification.

In the fourth experiment, which combined Procedure C of the purification process with Procedure B of the saponification process, the bath temperature for purification was adjusted to 40°C. The results indicated the presence of only a minor fraction of Cer NS24. Since Cer NS24 exists only as a free lipid and is one of the more abundant Cers in human SC, it is an indicator that the extraction of free lipids and pellet washing was very effective. Cer NS19 is not a physiological Cer since it has an odd chain length. In our case, it was added as the internal standard for quantification. In contrast, Cers of the type OS and OdS were identified, specifically those with carbon chain lengths of 28, 30, and 32. Additionally, Cers type OP with 28 and 30 carbon chains were detected (but these are not very common even among the free lipids). The OH type Cers were observed with a broader range of carbon chain lengths, including 28, 30, 32, 34, and 36 carbon atoms [Figure 10].

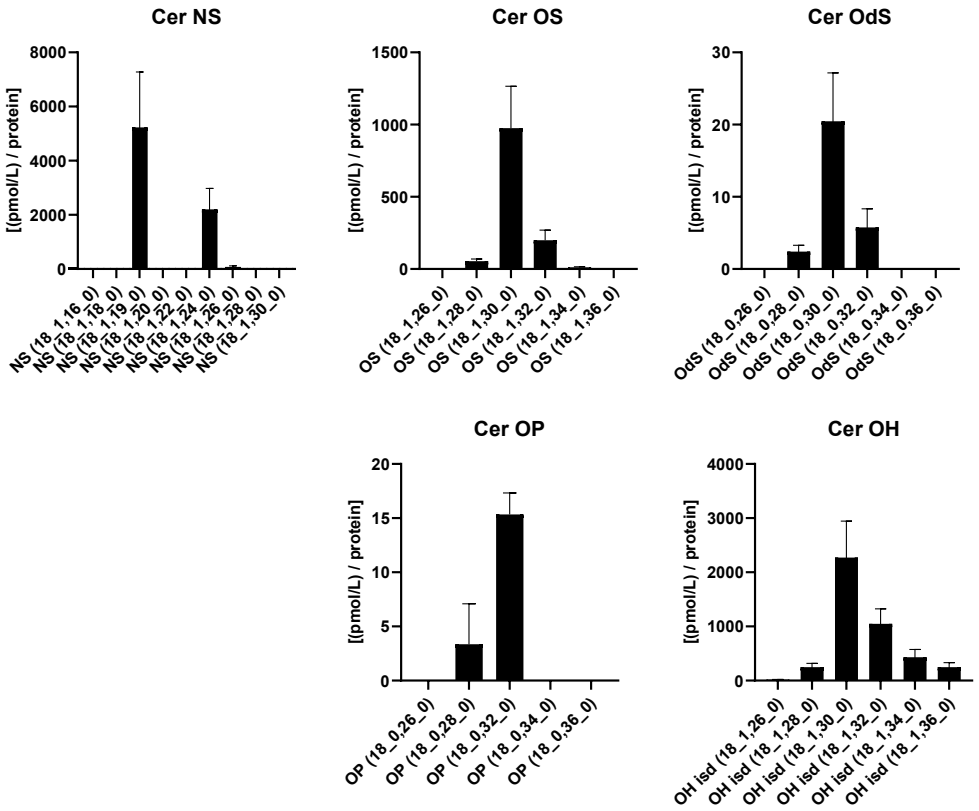

Figure 10. quantification of the lipids from the fourth experiment

These findings suggest that the modified bath temperature during purification enabled the isolation of covalently bound lipids, and we were able to quantify most of the expected Cer species. Moreover, we confirmed that the issue in the previous experiments was really the decomposition under high temperatures.

The fifth experiment, which combined Procedure C of the purification process with Procedure B of the saponification process, introduced variations in bath temperature during purification (adjusted to 45°C) and saponification (performed at 40°C and 50°C for two hours). As observed in Figure 11, the increased bath temperature to 50°C during saponification resulted in noticeable damage to the internal standard and other free lipids, indicating that this temperature was too harsh and led to the degradation of these components. Despite this, some free lipids, specifically NS types with carbon chain lengths of 16, 22, 26, and 28, remained in the final saponified samples, suggesting that the extraction process was not fully effective, even though the internal standard was compromised. Regarding Cer species, the OS type Cers displayed a strong reduction in the 50°C environment compared to the 40°C condition (however not statistically significant). Specifically, the OS 30 Cers were more abundant at 40°C, but their levels were notably lower than those observed in the fourth experiment, which was also conducted at 40°C. This suggests that even minor temperature increases from 37°C to 40°C can adversely affect these Cers. The OdS 30 Cers were similarly impacted, with their quantities decreasing by twofold at 40°C and fourfold at 50°C compared to the fourth experiment, confirming their sensitivity to heat. Interestingly, the OP 32 Cers exhibited a reduction of approximately 60% compared to the fourth experiment; however, there was no significant difference between the 40°C and 50°C conditions, indicating that these Cers are affected by heat but not further diminished within this specific temperature range. Conversely, the OH type Cers were relatively stable, as the temperature modifications did not strongly affect their levels compared to the fourth experiment. This suggests that OH Cers are more resistant to thermal degradation, which could be advantageous in certain applications.

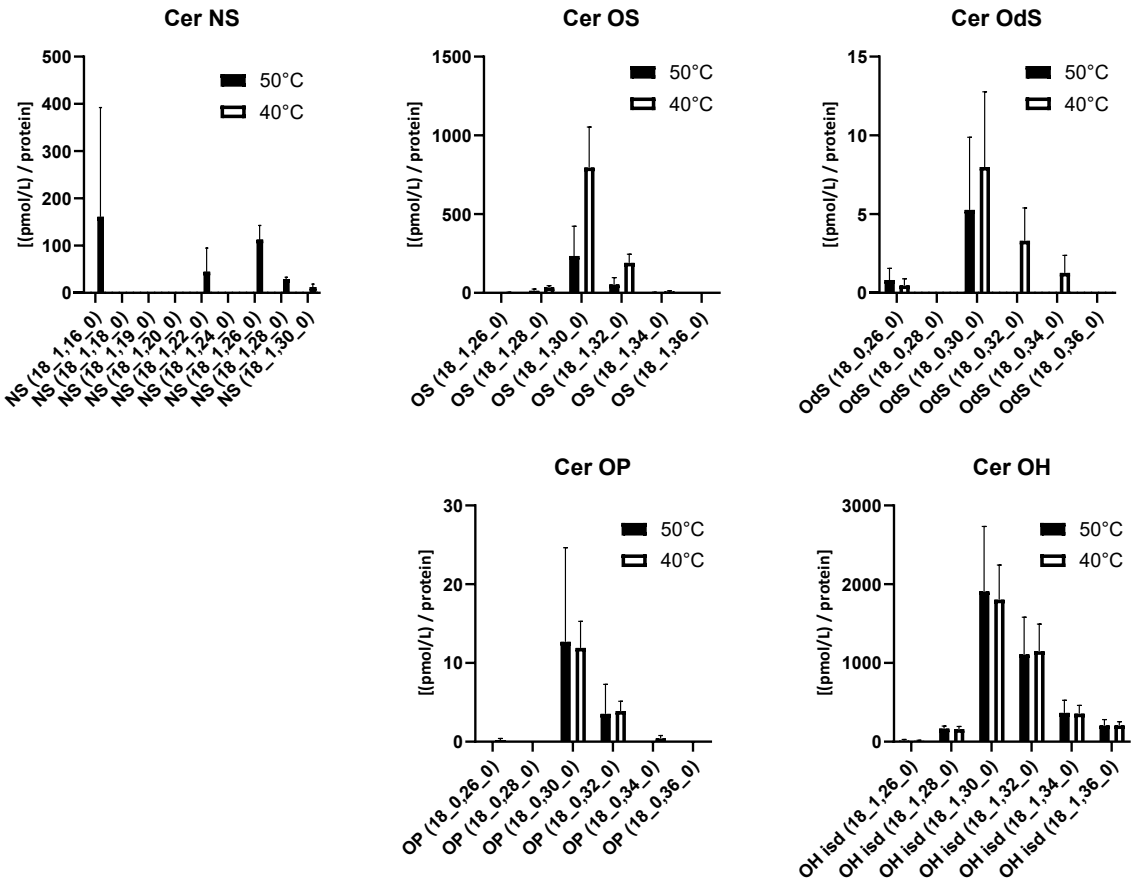

Figure 11. Quantified lipid results from the experiment No. 5. The differences between 40°C and 50°C were not statistically different

In conclusion, the fifth experiment underscores the critical role of temperature control in maintaining the stability and distribution of Cer species. The findings highlight the sensitivity of specific Cers, such as OS and OdS types, to temperature increases, while also revealing the limitations of the extraction process used, as evidenced by the remaining free lipids. This information suggested that the optimal way would be an increase in extraction time rather than an increase in temperature. The relative stability of OH Cers further emphasizes the importance of understanding the thermal properties of different Cer types in optimizing purification and saponification processes.

The sixth experiment, combining Procedure C of the purification process with Procedure B of the saponification process, introduced variations in washing time (4 or 8 hours) and saponification time (1.5 or 2 hours), while maintaining the saponification temperature at 37°C. According to Figure 12, a low quantity of free lipids (NS types) was detected, indicating their efficient removal. Surprisingly, the highest content of NS Cer was

detected with 8 hours of washing, indicating that a longer washing time even has increased the quantity of free lipids while our goal was a better washing of these lipids to have more pure final samples from the free lipids. However, in the context of the seventh experiment (described later), it seems more like a random deviation in the measurement. Unfortunately, calculating the statistical significance, in this case, is impossible since NS Cer was not found in all samples. For OS Cers with 30 and 32 carbon chains, these were most abundant after 2 hours of saponification. When compared to the fifth experiment at 40°C, longer saponification times significantly improved lipid solubilization, nearly doubling the amount compared to shorter saponification times. Similarly, OS Cers with 28 and 34 carbon chains were found in higher quantities with extended saponification, further confirming the positive impact on extraction efficiency.

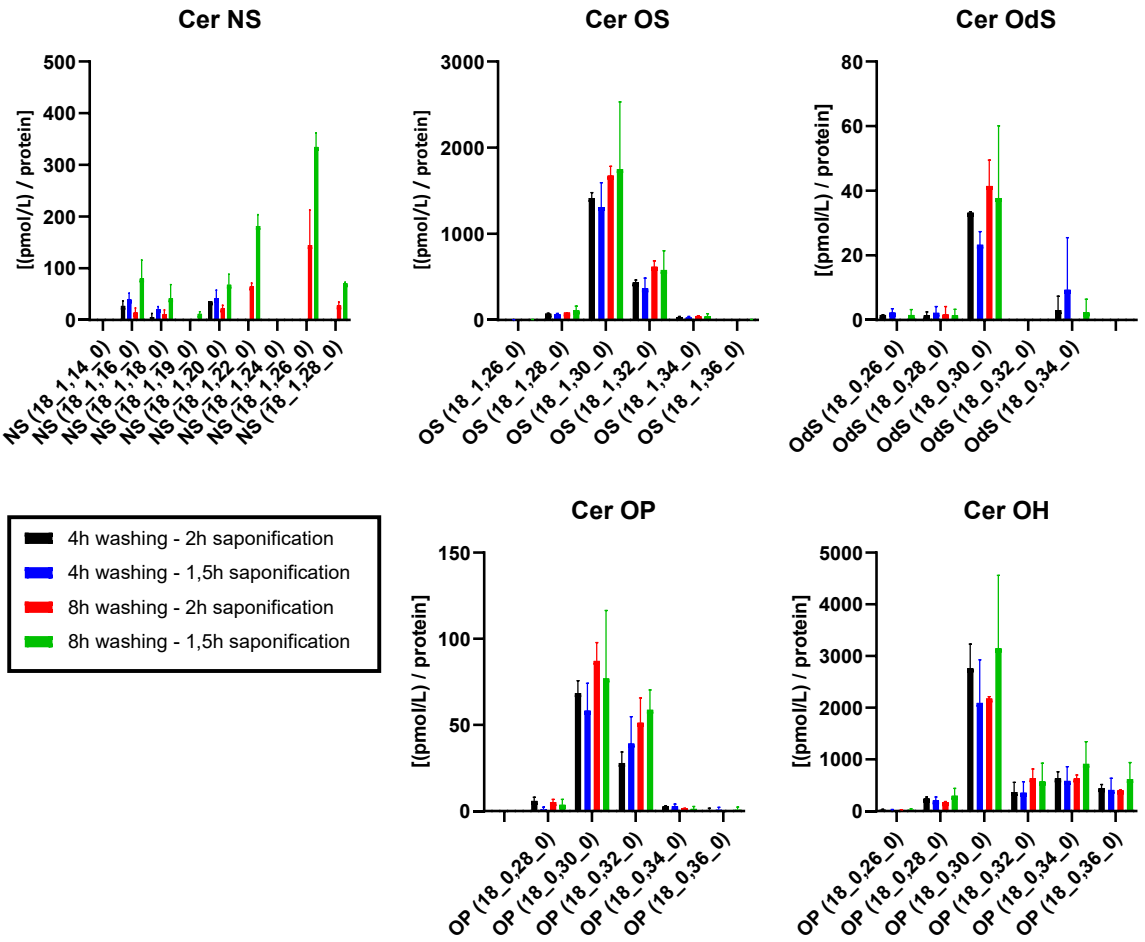

Figure 12. Quantified lipids resulted from the 6th experiment. Due to the complexity, the statistically significant differences were not indicated in the graph

For OdS Cers with 30 carbon chains, their quantity increased by 4 to 5 times compared to the fifth experiment, highlighting the effectiveness of prolonged saponification. This suggests that extended saponification positively influences the optimization of lipid extraction and quantification. Regarding OP Cers (30 carbon chains), extended saponification also enhanced extraction. However, for OP 32 Cers, shorter saponification surprisingly led to increased quantities of these Cers. Finally, OH 30 Cers were found in higher quantities when 1.5 hours of saponification was used, indicating that specific saponification durations can influence yield. Other O-type Cers showed minimal changes compared to the fifth experiment, underscoring the importance of optimizing saponification conditions, particularly for O-type Cers.

In the seventh experiment, we continued to combine Procedure C of the purification process with Procedure B of the saponification process, building on the findings from the sixth experiment and adjusting the washing times accordingly, as indicated by the results in Figure 13. The analysis indicates that the quantity of NS Cers 22 after overnight washing showed a statistically significant decrease compared to the three hours washing, with a p-value of less than 0.05, suggesting that the difference observed is likely real and not due to chance. For NS Cers 26, the effect was even more pronounced; the quantity after three hours of washing was significantly higher with a p-value of less than 0.0001, indicating a very strong difference from the overnight sample. Additionally, the five-hour washing also showed a highly statistically significant difference compared to overnight washing, further confirming a substantial effect of the washing length.

The analysis of Cer OS 30 reveals that washing the sample for 3 hours caused a statistically significant reduction in the quantity of this lipid when compared to the overnight sample. This indicates a strong and likely real difference in lipid quantity due to the shorter washing time. However, when the washing duration was extended to 7 hours, the difference in lipid quantity compared to the overnight sample was still statistically significant but less pronounced. The analysis of Cer OdS 34 indicates that the quantity of this lipid after washing was significantly decreased from the overnight sample. The analysis reveals that for Cer OP 30, washing the sample for 3 hours led to an extremely significant difference (increase) in lipid quantity compared to the overnight

sample, indicating a very strong effect. The 7 hours washing also showed a statistically significant difference, though the impact was less pronounced than the 3-hour washing. Additionally, in the case of Cer OP 32, the 3 hours washing resulted in a statistically significant difference compared to overnight washing. The analysis of Cer OH 30 indicates that only the 3 hours of washing resulted in a statistically significant difference (again an increase) in lipid quantity compared to the overnight washing, suggesting a meaningful impact from the shorter washing duration. In the case of Cer OH 32, the 3 hours of washing also produced a statistically significant difference, but with a p-value of less than 0.05, indicating a less pronounced effect compared to Cer OH 30. These results imply that the 3-hour washing significantly affects the lipid levels of both Cer OH 30 and Cer OH 32, though the effect is stronger in Cer OH 30.

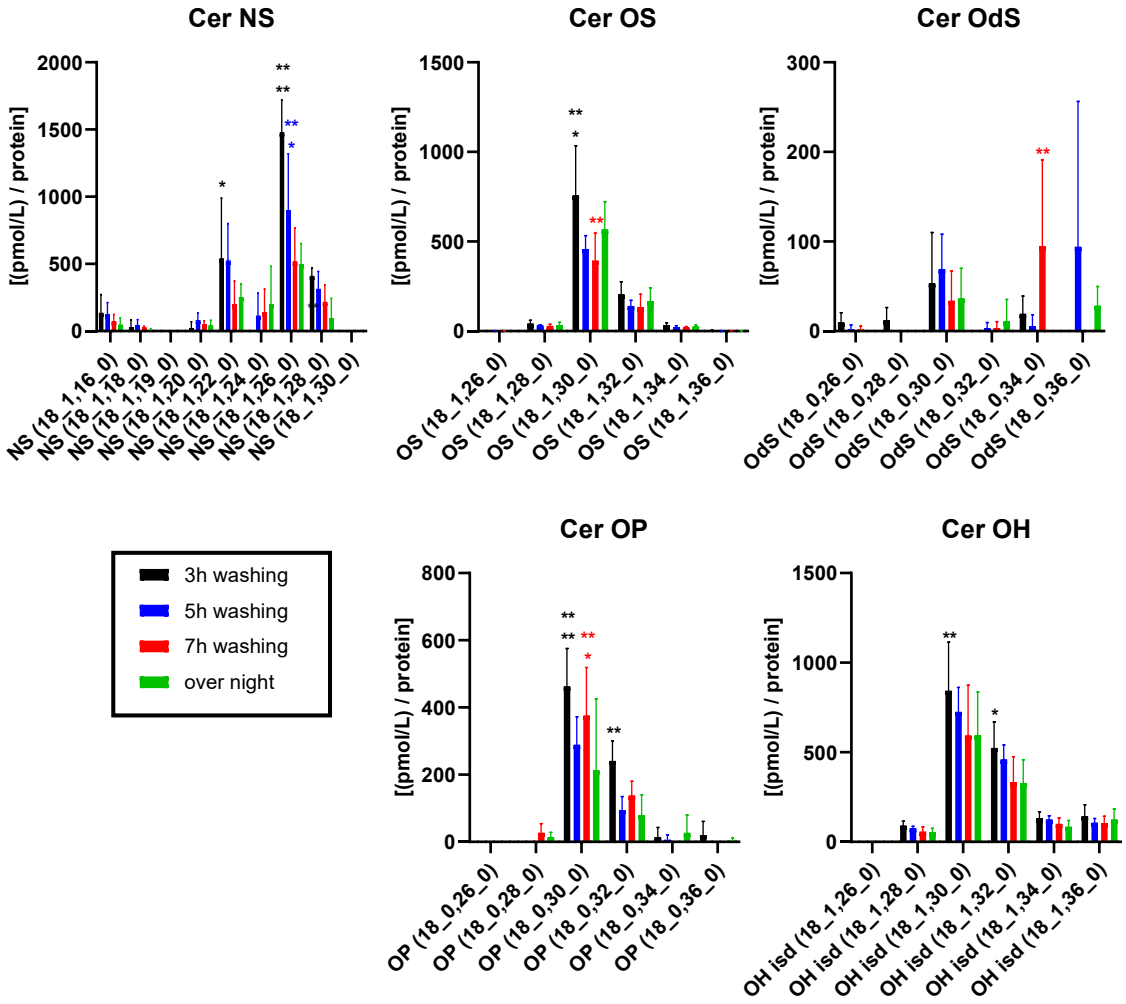

*Figure 13. Quantified lipids from the 7th experiment. Asterisks indicate statistically significant differences compared with the "overnight" sample at *, P < 0.05; **, P < 0.01; ***, P < 0.001; and ****, P < 0.0001*

The findings highlight that the shorter washing duration has a notable impact on the lipid quantities in these Cers. Thus, in potential further experiments, it is not reasonable to extend the washing times to over several hours. Overnight washing seems to reduce the amount of covalently bound lipids gained by this procedure.

In summary, the series of experiments demonstrated that temperature control and washing/saponification time are critical factors in optimizing the isolation of covalently bound lipids. High temperatures, as observed in the first and third experiments, were detrimental to both free and covalently bound lipids, leading to almost complete degradation. By lowering the saponification temperature and adjusting washing times, as in the fourth through seventh experiments, we achieved more effective lipid extraction, particularly for Cer types like OS, OdS, and OP. The results highlight that extended washing times, coupled with moderate temperatures, generally enhance lipid yield, though the optimal conditions vary depending on the specific Cer type. Ultimately, the findings suggest that precise control over both temperature and washing/saponification duration is essential for maximizing lipid recovery while minimizing degradation.

Based on the results of these experiments, the combination of Purification Procedure C with Saponification Procedure B appears to be the most effective. This conclusion is drawn from the observation that, after 5 hours of free lipid washing at 40°C followed by 2 hours of saponification at 37°C, there was a strong increase in the quantity of certain Cers, particularly OS Cers with 30 and 32 carbon chains, which were most abundant under these conditions.

4 MATERIALS AND METHODS

4.1 Materials

All chemicals, solvents and disposable materials used in this diploma project were purchased from suppliers like Merck (Darmstadt, Germany), VWR (Stříbrná skalice, Czech Republic), Penta (Prague, Czech Republic) and were used without further purification. All the solvents that were used for analysis were LC-MS^2 grade.

4.2 Preparation of human skin sample

4.2.1 Tape stripping

Samples of human skin were obtained from healthy donors based on informed written consent. The study was approved by an Ethical committee of Motol Hospital, Prague and was conducted according to the Helsinki Declaration. The tape (D-squame, 22 mm diameter, Dallas, USA) was placed on a suitable area of human skin (preferably the forearm) and pressed for approximately 3 seconds with mild pressure with the help of a D-Squame pressure device.

Eight strips (8 skin layers) were taken from the same spot on the human skin. After tape removal using tweezers on the non-sticky part of the tape, the tape was placed directly into 2 mL Eppendorf tubes for transport or storage. After transport/storage, tapes were carefully removed from Eppendorf tubes and transferred to the holder from the Squamescan tool (Dallas, USA).

For each study, we added two unused tapes as control. (Together 10 tapes from one individual)

4.2.2 Protein content measurement

Before measurement, the device was left running for 5 minutes. To make sure the instrument was working fine, calibration was performed using a holder consisting of one empty hole to zero the instrument and one with a defined value. After the test passed successfully with a deviation of 0.3, we continued.

The instrument was set to zero on one of the empty tapes and the difference between the two references was not more than 0.3. Then the rest of the samples from one patient were measured and the value was written down for data normalization. The instrument provides results as the % of infrared absorbance at the wavelength of 850 nm.

4.3 Internal standard preparation

Internal standard contains the following ceramides: NS (18:1/19:0), NS NS (18:1/31:0), OS (18:1/29:0), (OP 18:0/29:0), (OdS 18:0/29:0)

Individual Cers were dissolved in $CHCl_3$/MeOH 1:9 and then diluted with MeOH to reach a final concentration of 2 µmol/l.

50 µL of individual ceramide/base solutions were mixed and filled up to 5 mL with MeOH (4750 µL of MeOH). The final internal standard concentration was then 0.2 nmol/10 mL (= 20 nmol/l). 100 µL of the internal standard solution was then added to each sample.

4.4 Extraction of free lipids (general procedure)

Always two samples (tapes) were placed into one test tube (15 mL) as low as possible with the help of tweezers. Tapes should not overlap in order to have complete contact with the solution later.

The test tube was filled with 8 mL of the solvent, $CHCl_3$/MeOH/Water 30:60:8 and was shaken overnight at room temperature. Then, the test tubes were centrifuged at 3500 rpm for 10 minutes, and approximately 7 mL of the supernatant was collected via a syringe and added into the second test tube for evaporation. The content of the second test tube was evaporated to dryness under a gentle stream of nitrogen (it yields a white coating in the tip of the test tube). The pellet containing the residue of SC with covalently bound lipids and the residue of the tape remained in the original test tube.

To the remaining pellet, 7 mL of solvent ($CHCl_3$/MeOH/Water 30:60:8) was added. The samples were then sonicated for 3 minutes at 45°C followed by 12 minutes of incubation in a water bath. Afterward, the samples were centrifuged at 3500 rpm for 10 minutes. 7

mL of the supernatant was transferred into the second test tube and evaporated together using a gentle stream of nitrogen.

1.5 mL of $CHCl_3$/MeOH (1:9) was added into the test tube and the test tube was sonicated for a short time duration (approx. 30 seconds) at room temperature and then shortly vortexed. The content of the test tube was collected using a plastic syringe (2 mL) with a long cannula and filtered through a filter (PTFE, 13 mm diameter, 0.2 µm pores) into a 1.5 mL vial. The sample can be stored in the freezer at any stage of the procedure in order to keep them for the next time. For the measurement, 250 µL of this sample was transferred into another vial containing an insert (300 µL).

4.5 Purification of the pellet after the extraction of free lipids

4.5.1 Procedure A

To the residual pellet from the extraction of free lipids, 1 mL of MeOH was added, and the pellet was washed with three times 500 µL of MeOH in an ultra-sonic bath (40 °C, 15 min), centrifuged (6000 rpm, 5 min, tabletop centrifuge at room temperature) and the supernatant was collected in a separate vial. Then, the pellet was washed with two times 500 µL of MeOH in an ultra-sonic bath (60 °C, 2 h), centrifuged (6000 rpm, 5 min, tabletop centrifuge at room temperature) and the supernatant was discarded following collection. The washed pellet was then used for the saponification procedure.

4.5.2 Procedure B

The residual pellet was incubated with 500 µL of $CHCl_3$/MeOH (1:2, v/v) at 60°C for 3h and centrifuged (6000 rpm, room temperature, 10 minutes) to separate supernatant and pellet. The supernatant was collected, and 500 µL of $CHCl_3$/MeOH (1:2, v/v) was added to the pellet in the second round, and the same procedure was repeated. The third incubation was done according to the same procedure but for 16 h at 60 °C, then centrifuged, and the supernatant was collected and dried. The dried sample was mixed with 500 µL of $CHCl_3$/MeOH 1:9, vortexed and sonicated for 3 minutes in order to release the residue stuck on the vial. The sample was then centrifuged for 10 minutes at room temperature at 6000 rpm. 100 µL from the sample was transferred to vials to be

tested in LC-MS^2 (residual free lipids). The washed pellet was then used for the saponification procedure.

4.5.3 Procedure C

The resulting pellet was washed three times with 500 µL of MeOH, sonicated for 15 minutes at 40°C, and then centrifuged at 6000 rpm for 5 minutes to separate excess solvent. The supernatant was collected in a separate vial, and the washed pellet was then used for the saponification procedure.

4.6 Saponification of the covalently bound lipids

4.6.1 Procedure A (single-phase extraction)

100 µL of internal standard was added to the pellet, mixed and dried with a gentle nitrogen stream. Then, 200 µL of 1M KOH in 95% MeOH was added to the pellet, and the mixture was incubated for 2 h at 60°C in an ultra-sonic bath. After incubation, 200 µL of 1M acetic acid in MeOH was added to neutralize the extract, suspension was centrifuged (6000 rpm, 5 min, tabletop centrifuge at room temperature), the supernatant was collected in a separate vial and was dried under a gentle nitrogen stream.

For the desalting process, 1.2 mL water was added and suspended in the ultra-sonic bath at room temperature for 3 minutes. The suspension was transferred to RP-18 cartridges (Supelco, Darmstadt, Germany), samples were washed 3 times with 2 mL water, then vials were changed, and columns were washed two times with 2 mL methanol and once with 2 mL isopropanol. Vials with organic solvent were dried under the gentle stream of nitrogen in an evaporator.

2 mL of solvent ($CHCl_3$/MeOH 1:9) were added to the vials. Vials were under sonication for 3 minutes at room temperature. Then they were vortexed and filtered (PTFE, 13 mm diameter, 0.2 um pores) into 2 mL vials prepared for LC-MS^2.

4.6.2 Procedure B (two-phase extraction)

The pellets were suspended in 100 µL H_2O, 375 µL $CHCl_3$/MeOH 1:2 and mixed with 100 µL of internal standard. Then, the samples were treated with 50 µL 3 M KOH and

incubated at 37-50°C for 1-2 h (temperature and time depended on the particular experiment, with or without a sonication for the initial 5 min. 60 µL of 3 M formic acid along with 250 µL of $CHCl_3$ and 250 µL of water were added, and the whole amount of sample was transferred to a 1.5 mL Eppendorf tube using an automatic pipet. Samples then were centrifuged (13400 rpm, room temperature, 5 minutes) to separate the phases. The lower (organic) phase was collected using a syringe with a long cannula and dried in the vacuum evaporator (SpeedVac SPD300DDA, Thermo Scientific, Waltham, USA). The dried lipids were dissolved in 250 µL of $CHCl_3$/methanol (1:9, v/v), centrifuged at 13000 rpm for 10 minutes, and the supernatant was collected and filtered using PTFE filters (13 mm diameter, 0.2 um pores) into 2 mL vials and analyzed using LC-MS^2.

4.6.3 Procedure C (two-phase extraction)

The pellets were each suspended in 500 µL of 1 M KOH in 95% MeOH containing 100 µL of internal standard. Then, they were incubated at 60°C for 1 h. The samples were neutralized with 500 µL of 1 M acetic acid and mixed with 1 mL of $CHCl_3$ and 1.5 mL of H_2O successively. Then they were centrifuged at 6000 rpm, room temperature for 10 minutes, and the 1 mL of the organic phase was collected using a syringe with a long cannula across the samples, dried under a gentle nitrogen steam and dissolved in 500 µL of $CHCl_3$/methanol 1:9, vortexed and sonicated for 3 minutes in order to remove the residue on the test tube. They were then centrifuged for 10 minutes at room temperature at 6000 rpm followed by centrifugation for 10 minutes at 13400 rpm. The supernatant was collected in a separate vial. Finally, 100 µL from the sample was transferred to vials to be tested in LC-MS^2.

4.7 LC-MS/MS analysis

Cers were analyzed using the Shimadzu prominence HPLC instrument and Shimadzu LC-MS^2 8050 instrument (both Shimadzu, Japan). Cers were separated on a 15 cm Ascentis C18 column (15 cm × 2.1 mm; 3 µm, Supelco, USA) using a gradient between 57 % solvent A (50 % MeOH, 50 % water) and 99 % solvent B (99 % isopropanol, 1 % MeOH), both containing 10 mM ammonium formate and 0.1 % formic acid as additives at a flow rate of 0.2 mL/min at 30°C. Lipids analyzed via LC-MS^2 were detected using

multi-reaction monitoring (MRM). The quantification was performed based on the previously mentioned internal standards. Sphingoid bases were purchased from Avanti Polar Lipids (Alabaster, USA), and Cers were prepared by a direct acylation of sphingoid bases with appropriate fatty acids using *N*-(3-dimethylaminopropyl)-*N*′-ethylcarbodiimide and 1-hydroxybenzotriazole hydrate. For quantification, the correction for increasing sphingolipid chain length was taken into account.

4.8 Data evaluation

All data are presented as mean ± SD. Two-way ANOVA with Dunnett's post hoc test (indicated with * in the figures) was used for the statistical analysis, and $P < 0.05$ was considered significant. The data were normalized relative to protein concentration, with the results expressed in arbitrary units per protein concentration. All statistical tests were performed in GraphPad Prism® software 9.1.2 (GraphPad Prism, USA). Data acquisition and data processing were performed by using LabSolution LC-MS^2 software ver. 5.93 (Shimadzu, Kyoto, Japan). Both biological and chemical blank samples were prepared.

5 TABLE OF ABBREVIATIONS

Abbreviation	Description
12R-LOX	12R-lipoxygenase
A	α-hydroxy
AcylCer	Acylceramide
AD	Atopic Dermatitis
AI	Acquired Ichthyosis
ARCI	Autosomal Recessive Congenital Ichthyosis
Cer	Ceramide
CerS3	Cer synthase 3
$CHCl_3$	Chloroform
CHOL	Cholesterol
CLE	Corneocyte Lipid Envelope
DS	Dihydrosphingosine
EFA	Essential Fatty Acid
EFAD	Essential Fatty Acid Deficiency
eLOX3	Epidermal Lipoxygenase-3
EO	Esterified ω-hydroxy
FA	Fatty Acyl
FFA	Free Fatty Acid
GBA	Glucocerebrosidase
GlcCer	Glucosylceramide
H	6-hydroxysphingosine
LA	Linoleic Acid
LCB	Long Chain Base
LC-MS	Liquid Chromatography - Mass Spectrometry
LPP	Long Periodicity Phase
MeOH	Methanol
N	Nonhydroxy FA
O	ω-hydroxy FA
P	Phytosphingosine
S	Sphingosine

SC	Stratum Corneum
SD	Sphingadiene
SM	Sphingomyelin
SPP	Short Periodicity Phase
STS	Steroid Sulfatase
TEWL	Transepidermal Water Loss

6 REFERENCES

1. Ishikawa, J., et al., *Changes in the ceramide profile of atopic dermatitis patients.* Journal of Investigative Dermatology, 2010. **130**(10): p. 2511.
2. Janssens, M., et al., *Increase in short-chain ceramides correlates with an altered lipid organization and decreased barrier function in atopic eczema patients [S].* Journal of lipid research, 2012. **53**(12): p. 2755-2766.
3. Tawada, C., et al., *Interferon-γ decreases ceramides with long-chain fatty acids: possible involvement in atopic dermatitis and psoriasis.* Journal of Investigative Dermatology, 2014. **134**(3): p. 712-718.
4. Castiel-Higounenc, I., M. Chopart, and C. Ferraris, *Stratum corneum lipids: specificity, role, deficiencies and modulation.* Oléagineux, Corps gras, Lipides, 2004. **11**(6): p. 401-406.
5. Byrd, A.L., Y. Belkaid, and J.A. Segre, *The human skin microbiome.* Nature Reviews Microbiology, 2018. **16**(3): p. 143-155.
6. Yosipovitch, G., et al., *Skin barrier damage and itch: review of mechanisms, topical management and future directions.* Acta dermato-venereologica, 2019. **99**(13): p. 1201-1209.
7. Wickett, R.R. and M.O. Visscher, *Structure and function of the epidermal barrier.* American journal of infection control, 2006. **34**(10): p. S98-S110.
8. Venus, M., J. Waterman, and I. McNab, *Basic physiology of the skin.* Surgery (Oxford), 2010. **28**(10): p. 469-472.
9. Meckfessel, M.H. and S. Brandt, *The structure, function, and importance of ceramides in skin and their use as therapeutic agents in skin-care products.* Journal of the American Academy of Dermatology, 2014. **71**(1): p. 177-184.
10. Van Smeden, J., et al., *The important role of stratum corneum lipids for the cutaneous barrier function.* Biochimica et Biophysica Acta (BBA)-Molecular and Cell Biology of Lipids, 2014. **1841**(3): p. 295-313.
11. de Jager, M.W., et al., *Lipid mixtures prepared with well-defined synthetic ceramides closely mimic the unique stratum corneum lipid phase behavior.* Journal of lipid research, 2005. **46**(12): p. 2649-2656.
12. Bouwstra, J., G. Gooris, and M. Ponec, *The lipid organisation of the skin barrier: liquid and crystalline domains coexist in lamellar phases.* Journal of biological physics, 2002. **28**: p. 211-223.
13. Pullmannová, P., et al., *Long and very long lamellar phases in model stratum corneum lipid membranes.* Journal of lipid research, 2019. **60**(5): p. 963-971.
14. Uchino, T., et al., *Comparative analysis of intercellular lipid organization and composition between psoriatic and healthy stratum corneum.* Chemistry and Physics of Lipids, 2023. **254**: p. 105305.
15. Berkers, T., et al., *Degree of skin barrier disruption affects lipid organization in regenerated stratum corneum.* Acta dermato-venereologica, 2018. **98**(4): p. 421-427.
16. Madison, K.C., *Barrier function of the skin:"la raison d'etre" of the epidermis.* Journal of investigative dermatology, 2003. **121**(2): p. 231-241.

17. Imokawa, G., et al., *Decreased level of ceramides in stratum corneum of atopic dermatitis: an etiologic factor in atopic dry skin?* Journal of Investigative Dermatology, 1991. **96**(4): p. 523-526.
18. Uchida, Y. and K. Park, *Ceramides in skin health and disease: an update.* American Journal of Clinical Dermatology, 2021. **22**(6): p. 853-866.
19. Kihara, A., *Synthesis and degradation pathways, functions, and pathology of ceramides and epidermal acylceramides.* Progress in lipid research, 2016. **63**: p. 50-69.
20. Pruett, S.T., et al., *Thematic Review Series: Sphingolipids. Biodiversity of sphingoid bases ("sphingosines") and related amino alcohols.* Journal of lipid research, 2008. **49**(8): p. 1621-1639.
21. Imokawa, G., et al., *Pseudo-acylceramide with linoleic acid produces selective recovery of diminished cutaneous barrier function in essential fatty acid-deficient rats and has an inhibitory effect on epidermal hyperplasia.* The Journal of clinical investigation, 1994. **94**(1): p. 89-96.
22. Motta, S., et al., *Ceramide composition of the psoriatic scale.* Biochimica et Biophysica Acta (BBA)-Molecular Basis of Disease, 1993. **1182**(2): p. 147-151.
23. Akiyama, M., *Corneocyte lipid envelope (CLE), the key structure for skin barrier function and ichthyosis pathogenesis.* Journal of dermatological science, 2017. **88**(1): p. 3-9.
24. Elias, P.M., et al., *Formation and functions of the corneocyte lipid envelope (CLE).* Biochimica et Biophysica Acta (BBA)-Molecular and Cell Biology of Lipids, 2014. **1841**(3): p. 314-318.
25. Marekov, L.N. and P.M. Steinert, *Ceramides are bound to structural proteins of the human foreskin epidermal cornified cell envelope.* Journal of Biological Chemistry, 1998. **273**(28): p. 17763-17770.
26. Muñoz-Garcia, A., et al., *The importance of the lipoxygenase-hepoxilin pathway in the mammalian epidermal barrier.* Biochimica et Biophysica Acta (BBA)-Molecular and Cell Biology of Lipids, 2014. **1841**(3): p. 401-408.
27. Kawana, M., et al., *Comparative profiling and comprehensive quantification of stratum corneum ceramides in humans and mice by LC/MS/MS [S].* Journal of lipid research, 2020. **61**(6): p. 884-895.
28. Masukawa, Y., et al., *Characterization of overall ceramide species in human stratum corneums.* Journal of lipid research, 2008. **49**(7): p. 1466-1476.
29. Grösch, S., S. Schiffmann, and G. Geisslinger, *Chain length-specific properties of ceramides.* Progress in lipid research, 2012. **51**(1): p. 50-62.
30. Opalka, L., et al., *Scalable synthesis of human ultralong chain ceramides.* Organic Letters, 2015. **17**(21): p. 5456-5459.
31. Leal, A.F., et al., *Sphingolipids and their role in health and disease in the central nervous system.* Advances in Biological Regulation, 2022. **85**: p. 100900.
32. Hamanaka, S., et al., *Glucosylceramide accumulates preferentially in lamellar bodies in differentiated keratinocytes.* British Journal of Dermatology, 2005. **152**(3): p. 426-434.
33. Amalia, L. and S.-L. Tsai, *Ceramide's Role and Biosynthesis: A Brief Review.* Biotechnology and Bioprocess Engineering, 2023: p. 1-8.

34. Gault, C.R., L.M. Obeid, and Y.A. Hannun, *An overview of sphingolipid metabolism: from synthesis to breakdown.* Sphingolipids as signaling and regulatory molecules, 2010: p. 1-23.
35. Rao, B.D., P. Sarkar, and A. Chattopadhyay, *Metabolic Depletion of Sphingolipids Does Not Alter Cell Cycle Progression in Chinese Hamster Ovary Cells.* The Journal of Membrane Biology, 2022. **255**(1): p. 1-12.
36. van Meer, G. and Q. Lisman, *Sphingolipid transport: rafts and translocators.* Journal of Biological Chemistry, 2002. **277**(29): p. 25855-25858.
37. Ishibashi, Y., A. Kohyama-Koganeya, and Y. Hirabayashi, *New insights on glucosylated lipids: metabolism and functions.* Biochimica et Biophysica Acta (BBA)-Molecular and Cell Biology of Lipids, 2013. **1831**(9): p. 1475-1485.
38. Freinkel, R.K. and T.N. Traczyk, *A method for partial purification of lamellar granules from fetal rat epidermis.* Journal of Investigative Dermatology, 1981. **77**(6): p. 478-482.
39. Grayson, S., et al., *Lamellar body-enriched fractions from neonatal mice: preparative techniques and partial characterization.* Journal of investigative dermatology, 1985. **85**(4): p. 289-294.
40. Madison, K.C., et al. *Lamellar granule biogenesis: a role for ceramide glucosyltransferase, lysosomal enzyme transport, and the Golgi*. in *Journal of Investigative Dermatology Symposium Proceedings*. 1998. Elsevier.
41. Jakobsson, A., R. Westerberg, and A. Jacobsson, *Fatty acid elongases in mammals: their regulation and roles in metabolism.* Progress in lipid research, 2006. **45**(3): p. 237-249.
42. Vasireddy, V., et al., *Loss of functional ELOVL4 depletes very long-chain fatty acids (≥ C28) and the unique ω-O-acylceramides in skin leading to neonatal death.* Human molecular genetics, 2007. **16**(5): p. 471-482.
43. Esperón-Moldes, U., et al., *Novel CYP4F22 mutations associated with autosomal recessive congenital ichthyosis (ARCI). Study of the CYP4F22 c. 1303C> T founder mutation.* PLoS One, 2020. **15**(2): p. e0229025.
44. Ohno, Y., et al., *Essential role of the cytochrome P450 CYP4F22 in the production of acylceramide, the key lipid for skin permeability barrier formation.* Proceedings of the National Academy of Sciences, 2015. **112**(25): p. 7707-7712.
45. Mizutani, Y., et al., *Ceramide biosynthesis in keratinocyte and its role in skin function.* Biochimie, 2009. **91**(6): p. 784-790.
46. Johnson, A.L., et al., *Cytochrome P450 ω-hydroxylases in inflammation and cancer.* Advances in pharmacology, 2015. **74**: p. 223-262.
47. Pichery, M., et al., *PNPLA1 defects in patients with autosomal recessive congenital ichthyosis and KO mice sustain PNPLA1 irreplaceable function in epidermal omega-O-acylceramide synthesis and skin permeability barrier.* Human Molecular Genetics, 2017. **26**(10): p. 1787-1800.
48. Elias, P.M., B.E. Brown, and V.A. Ziboh, *The permeability barrier in essential fatty acid deficiency: evidence for a direct role for linoleic acid in barrier function.* Journal of Investigative Dermatology, 1980. **74**(4): p. 230-233.
49. Gramlich, L., et al., *Essential fatty acid requirements and intravenous lipid emulsions.* Journal of Parenteral and Enteral Nutrition, 2019. **43**(6): p. 697-707.

50. De Meijer, V.E., et al., *Parenteral fish oil as monotherapy prevents essential fatty acid deficiency in parenteral nutrition–dependent patients.* Journal of pediatric gastroenterology and nutrition, 2010. **50**(2): p. 212-218.
51. Akiyama, M., *Acylceramide is a key player in skin barrier function: insight into the molecular mechanisms of skin barrier formation and ichthyosis pathogenesis.* The FEBS Journal, 2021. **288**(7): p. 2119-2130.
52. Breiden, B. and K. Sandhoff, *The role of sphingolipid metabolism in cutaneous permeabilitybarrier formation.* Biochimica et Biophysica Acta (BBA)-Molecular and Cell Biology of Lipids, 2014. **1841**(3): p. 441-452.
53. Opálka, L.s., et al., *Omega-O-acylceramides in skin lipid membranes: effects of concentration, sphingoid base, and model complexity on microstructure and permeability.* Langmuir, 2016. **32**(48): p. 12894-12904.
54. Takagi, Y., et al., *Biosynthesis of acylceramide in murine epidermis: characterization by inhibition of glucosylation and deglucosylation, and by substrate specificity.* Journal of investigative dermatology, 2004. **122**(3): p. 722-729.
55. Mashima, R. and T. Okuyama, *The role of lipoxygenases in pathophysiology; new insights and future perspectives.* Redox biology, 2015. **6**: p. 297-310.
56. Tyrrell, V.J., et al., *Lipidomic and transcriptional analysis of the linoleoyl-omega-hydroxyceramide biosynthetic pathway in human psoriatic lesions.* Journal of Lipid Research, 2021. **62**.
57. Noguchi, S., et al., *Evaluation of ω-alkynyl-labeled linoleic and arachidonic acids as substrates for recombinant lipoxygenase pathway enzymes.* Biochimica et Biophysica Acta (BBA)-Molecular and Cell Biology of Lipids, 2023. **1868**(9): p. 159360.
58. Takeichi, T., et al., *SDR9C7 catalyzes critical dehydrogenation of acylceramides for skin barrier formation.* The Journal of Clinical Investigation, 2020. **130**(2): p. 890-903.
59. Sayre, L.M., et al., *Pyrrole formation from 4-hydroxynonenal and primary amines.* Chemical research in toxicology, 1993. **6**(1): p. 19-22.
60. Sayre, L.M., et al., *Protein adducts generated from products of lipid oxidation: focus on HNE and one.* Drug metabolism reviews, 2006. **38**(4): p. 651-675.
61. Wertz, P., *Current understanding of skin biology pertinent to skin penetration: skin biochemistry.* Skin pharmacology and physiology, 2013. **26**(4-6): p. 217-226.
62. Christoffersen, C., et al., *Endothelium-protective sphingosine-1-phosphate provided by HDL-associated apolipoprotein M.* Proceedings of the National Academy of Sciences, 2011. **108**(23): p. 9613-9618.
63. Kitatani, K., J. Idkowiak-Baldys, and Y.A. Hannun, *The sphingolipid salvage pathway in ceramide metabolism and signaling.* Cellular signalling, 2008. **20**(6): p. 1010-1018.
64. Uchida, Y. and W.M. Holleran, *Omega-O-acylceramide, a lipid essential for mammalian survival.* Journal of dermatological science, 2008. **51**(2): p. 77-87.
65. Dorf, I.L., et al., *Validity of First-Time Diagnoses of Darier's Disease in the Danish National Patient Registry.* Clinical epidemiology, 2021: p. 1063-1069.

66. Park, J.S., et al., *Inherited ichthyosis as a paradigm of rare skin disorders: genomic medicine, pathogenesis, and management.* Journal of the American Academy of Dermatology, 2022.
67. Thyssen, J., E. Godoy-Gijon, and P. Elias, *Ichthyosis vulgaris: the filaggrin mutation disease.* British journal of dermatology, 2013. **168**(6): p. 1155-1166.
68. Akiyama, M., *FLG mutations in ichthyosis vulgaris and atopic eczema: spectrum of mutations and population genetics.* British Journal of Dermatology, 2010. **162**(3): p. 472-477.
69. Compton, J.G., et al., *Mapping of the associated phenotype of an absent granular layer in ichthyosis vulgaris to the epidermal differentiation complex on chromosome 1.* Experimental dermatology, 2002. **11**(6): p. 518-526.
70. Zhong, W., et al., *Linkage analysis suggests a locus of ichthyosis vulgaris on 1q22.* Journal of human genetics, 2003. **48**(7): p. 390-392.
71. Smith, F.J., et al., *Loss-of-function mutations in the gene encoding filaggrin cause ichthyosis vulgaris.* Nature genetics, 2006. **38**(3): p. 337-342.
72. Sandilands, A., et al., *Prevalent and rare mutations in the gene encoding filaggrin cause ichthyosis vulgaris and predispose individuals to atopic dermatitis.* Journal of Investigative Dermatology, 2006. **126**(8): p. 1770-1775.
73. Oji, V., et al., *Ichthyosis vulgaris: novel FLG mutations in the German population and high presence of CD1a+ cells in the epidermis of the atopic subgroup.* British Journal of Dermatology, 2009. **160**(4): p. 771-781.
74. Gruber, R., et al., *Filaggrin mutations p. R501X and c. 2282del4 in ichthyosis vulgaris.* European journal of human genetics, 2007. **15**(2): p. 179-184.
75. Sandilands, A., et al., *Comprehensive analysis of the gene encoding filaggrin uncovers prevalent and rare mutations in ichthyosis vulgaris and atopic eczema.* Nature genetics, 2007. **39**(5): p. 650-654.
76. Winge, M., et al., *Novel filaggrin mutation but no other loss-of-function variants found in Ethiopian patients with atopic dermatitis.* British Journal of Dermatology, 2011. **165**(5): p. 1074-1080.
77. Liu, P., et al., *Identification of a genetic locus for ichthyosis vulgaris on chromosome 10q22. 3–q24. 2.* Journal of investigative dermatology, 2008. **128**(6): p. 1418-1422.
78. Cockayne, E.A., *Inherited abnormalities of the skin and its appendages*, in *Inherited abnormalities of the skin and its appendages*. 1933. p. 394-394.
79. France, J.T., *Steroid sulphatase deficiency.* Journal of Steroid Biochemistry, 1979. **11**(1): p. 647-651.
80. Yen, P.H., et al., *The human X-linked steroid sulfatase gene and a Y-encoded pseudogene: evidence for an inversion of the Y chromosome during primate evolution.* Cell, 1988. **55**(6): p. 1123-1135.
81. Mueller, J.W., et al., *The regulation of steroid action by sulfation and desulfation.* Endocrine reviews, 2015. **36**(5): p. 526-563.
82. Fandrei, F., et al., *Cholesterol sulfate fluidizes the sterol fraction of the stratum corneum lipid phase and increases its permeability.* Journal of Lipid Research, 2022. **63**(3).

83. Elias, P.M., et al., *Role of cholesterol sulfate in epidermal structure and function: lessons from X-linked ichthyosis.* Biochimica et Biophysica Acta (BBA)-Molecular and Cell Biology of Lipids, 2014. **1841**(3): p. 353-361.
84. Oji, V., et al., *Revised nomenclature and classification of inherited ichthyoses: results of the First Ichthyosis Consensus Conference in Sorèze 2009.* Journal of the American Academy of Dermatology, 2010. **63**(4): p. 607-641.
85. Fartasch, M., *Epidermal barrier in disorders of the skin.* Microscopy research and technique, 1997. **38**(4): p. 361-372.
86. Ghadially, R., et al., *Membrane structural abnormalities in the stratum corneum of the autosomal recessive ichthyoses.* Journal of investigative dermatology, 1992. **99**(6): p. 755-763.
87. Paige, D., N. Morse-Fisher, and J. Harper, *Quantification of stratum corneum ceramides and lipid envelope ceramides in the hereditary ichthyoses.* British Journal of Dermatology, 1994. **131**(1): p. 23-27.
88. Lavrijsen, A.P., et al., *Reduced skin barrier function parallels abnormal stratum corneum lipid organization in patients with lamellar ichthyosis.* Journal of Investigative dermatology, 1995. **105**(4): p. 619-624.
89. Fischer, J., A. Hotz, and K. Komlosi, *Syndromic ichthyoses.* Medizinische Genetik, 2023. **35**(1): p. 23-32.
90. Schwartz, R. and M. Williams, *Acquired ichthyosis: a marker for internal disease.* American Family Physician, 1984. **29**(2): p. 181-184.
91. Homayoun, A., *Acquired ichthyosis and related conditions.* International journal of dermatology, 1984. **23**(7): p. 458-461.
92. DiGiovanna, J.J. and L. Robinson-Bostom, *Ichthyosis: etiology, diagnosis, and management.* American journal of clinical dermatology, 2003. **4**: p. 81-95.
93. Jordan, C.T., et al., *Rare and common variants in CARD14, encoding an epidermal regulator of NF-kappaB, in psoriasis.* The American Journal of Human Genetics, 2012. **90**(5): p. 796-808.
94. Tsoi, L.C., et al., *Identification of 15 new psoriasis susceptibility loci highlights the role of innate immunity.* Nature genetics, 2012. **44**(12): p. 1341-1348.
95. Puig, L., A. Julià, and S. Marsal, *The pathogenesis and genetics of psoriasis.* Actas Dermo-Sifiliográficas (English Edition), 2014. **105**(6): p. 535-545.
96. Zhang, X.-J., et al., *Psoriasis genome-wide association study identifies susceptibility variants within LCE gene cluster at 1q21.* Nature genetics, 2009. **41**(2): p. 205-210.
97. Sahle, F.F., et al., *Skin diseases associated with the depletion of stratum corneum lipids and stratum corneum lipid substitution therapy.* Skin pharmacology and physiology, 2015. **28**(1): p. 42-55.
98. Ahlström, M.G., et al., *Stratum Corneum Lipids in Non-Lesional Atopic and Healthy Skin following Moisturizer Application: A Randomized Clinical Experiment.* Life, 2024. **14**(3): p. 345.
99. Cork, M.J., et al., *New perspectives on epidermal barrier dysfunction in atopic dermatitis: gene–environment interactions.* Journal of Allergy and Clinical Immunology, 2006. **118**(1): p. 3-21.
100. Leung, D., A. Rhodes, and R. Geha, *et aJ. Atopic dermatitis.* Dermatology and general medicine. 3rd ed. New York: McGraw-Hill, 1986: p. 1385-408.

101. Di Nardo, A., et al., *Ceramide and cholesterol composition of the skin of patients with atopic dermatitis.* Acta dermato-venereologica, 1998. **78**: p. 27-30.
102. Elias, P.M. and M. Steinhoff, *"Outside-to-inside"(and now back to "outside") pathogenic mechanisms in atopic dermatitis.* Journal of Investigative Dermatology, 2008. **128**(5): p. 1067-1070.
103. Seidenari, S. and G. Giusti, *Objective assessment of the skin of children affected by atopic dermatitis: a study of pH, capacitance and TEWL in eczematous and clinically uninvolved skin.* Acta dermato-venereologica, 1995. **75**: p. 429-433.
104. Werner, Y. and M. Lindberg, *Transepidermal water loss in dry and clinically normal skin in patients with atopic dermatitis.* Acta dermato-venereologica, 1985. **65**(2): p. 102-105.
105. Yoshiike, T., et al., *Skin barrier defect in atopic dermatitis: increased permeability of the stratum corneum using dimethyl sulfoxide and theophylline.* Journal of dermatological science, 1993. **5**(2): p. 92-96.
106. Brown, S.J. and W.I. McLean, *One remarkable molecule: filaggrin.* Journal of Investigative Dermatology, 2012. **132**(3): p. 751-762.
107. Irvine, A.D., W.I. McLean, and D.Y. Leung, *Filaggrin mutations associated with skin and allergic diseases.* New England Journal of Medicine, 2011. **365**(14): p. 1315-1327.
108. Jakasa, I., et al., *Skin barrier function in healthy subjects and patients with atopic dermatitis in relation to filaggrin loss-of-function mutations.* Journal of investigative dermatology, 2011. **131**(2): p. 540.
109. O'Regan, G.M. and A.D. Irvine, *The role of filaggrin loss-of-function mutations in atopic dermatitis.* Current opinion in allergy and clinical immunology, 2008. **8**(5): p. 406-410.
110. Palmer, C., et al., *1: CAS: 528: DC% 2BD28XivFShtLo% 3D: Common loss-of-function variants of the epidermal barrier protein filaggrin are a major predisposing factor for atopic dermatitis. vol. 38.* Nat Genet, 2006: p. 441-446.
111. Bieber, T., *Atopic dermatitis N Engl J Med. 2008; 358: 1483–94 doi: 10.1056.* NEJMra074081.
112. Irvine, A.D., *Fleshing out filaggrin phenotypes.* Journal of Investigative Dermatology, 2007. **127**(3): p. 504-507.
113. Oyoshi, M.K., et al., *Cellular and molecular mechanisms in atopic dermatitis.* Advances in immunology, 2009. **102**: p. 135-226.
114. Danso, M., et al., *Altered expression of epidermal lipid bio-synthesis enzymes in atopic dermatitis skin is accompanied by changes in stratum corneum lipid composition.* Journal of dermatological science, 2017. **88**(1): p. 57-66.
115. Macheleidt, O., K. Sandhoff, and H.W. Kaiser, *Deficiency of epidermal protein-bound ω-hydroxyceramides in atopic dermatitis.* Journal of Investigative Dermatology, 2002. **119**(1): p. 166-173.
116. Hamanaka, S., et al., *Human epidermal glucosylceramides are major precursors of stratum corneum ceramides.* Journal of Investigative Dermatology, 2002. **119**(2): p. 416-423.
117. Holleran, W.M., et al., *Processing of epidermal glucosylceramides is required for optimal mammalian cutaneous permeability barrier function.* The Journal of clinical investigation, 1993. **91**(4): p. 1656-1664.

118. Uchida, Y., et al., *Epidermal sphingomyelins are precursors for selected stratum corneum ceramides.* Journal of lipid research, 2000. **41**(12): p. 2071-2082.
119. Suzuki, M., Y. Ohno, and A. Kihara, *Whole picture of human stratum corneum ceramides, including the chain-length diversity of long-chain bases.* Journal of Lipid Research, 2022. **63**(7).
120. Ohno, Y., et al., *Determining the structure of protein-bound ceramides, essential lipids for skin barrier function.* Iscience, 2023. **26**(11).